Relaxation dynamics in a lattice gas: A test of the mode-coupling theory of the ideal glass transition

Walter Kob and Hans C. Andersen
Department of Chemistry, Stanford University, Stanford, California 94305
(Received 23 September 1992)

By means of computer simulations we investigate the dynamical behavior of a binary lattice-gas mixture with short-range interactions in order to provide a stringent test of mode-coupling theory (MCT). The dynamics of the particles is given by Monte Carlo–like moves that change the positions of the particles and binary collisions that change the velocities. By monitoring the self part of the van Hove correlation function we find the low-temperature dynamics to be glasslike. In accordance with MCT, the imaginary part of the dynamic susceptibility χ'' shows a well-defined α peak whose high-frequency wing follows a von Schweidler law with an exponent that is independent of temperature. The low-frequency wing of the peak follows a different power-law dependence that corresponds to a power law of the form $-P+A/t^{\delta}$ $(A, P, \delta > 0)$ in the self part of the intermediate scattering function $F_{s1}(k,t)$. In agreement with MCT we find that the diffusion constant for one of the two types of particles, the relaxation times of $F_{s1}(k,t)$, the location of the α peak in the susceptibility, and the prefactor of the von Schweidler law all have a power-law dependence on temperature, $(T-T_c)^{\gamma}$, for $T > T_c$ at constant density. As predicted by the theory, the critical temperatures T_c for the different quantities are the same within the statistical error. However, in contradiction to MCT, the critical exponents γ vary from one quantity to another. The value of the Lamb-Mössbauer factor shows qualitatively the wave-vector dependence predicted by MCT. The self part of a second kind of correlation function exhibits the two power laws predicted by MCT for the high- and low-frequency wings of the β relaxation. We show that, in the vicinity of the minimum in χ'', the scaling behavior predicted by MCT holds. However, the location of this minimum at a given temperature depends on the quantity investigated, contrary to the predictions of MCT. Moreover, the value of χ'' at this minimum exhibits a power-law dependence on temperature with an exponent that is significantly larger than the one predicted by MCT. We also find that the height of the α peak as well as the total energy per particle have a power-law dependence on temperature and that the corresponding critical temperatures are close to those obtained for the other quantities.

PACS number(s): 61.20.Ja, 64.70.Pf, 51.10.+y, 05.20.−y

I. INTRODUCTION

In the 1970s mode-coupling approximations, originally applied by Kawasaki for the description of second-order phase transitions [1], were used successfully for the description of the dynamics of dense liquids [2, 3]. Later it was recognized that the solution of the equations resulting from the mode-coupling approximations, which are very similar to the equations obtained from the so-called fully renormalized kinetic theory for dense fluids [3, 4], can lead to singularities in transport coefficients and to a structural arrest if the system is cooled (or compressed) enough [5, 6]. Structural arrest means here that the intermediate scattering function $F(\mathbf{q},t) = \langle \rho_q(t)\rho_q(0)\rangle$ does not decay to zero in the long-time limit. Here $\rho_q(t)$ is the density fluctuation for wave vector $\mathbf{q}$ at time t and $\langle\,\rangle$ denotes the average over the canonical ensemble. This arrest happens at a critical temperature T_c (or a critical density n_c) at which the dynamics changes from ergodic to nonergodic. As the intrinsic structure of the liquid does not change significantly when the system is cooled from temperatures slightly above T_c to temperatures slightly below T_c, one ends up with a frozen liquid, i.e., a glass. Thus T_c was tentatively identified with the calorimetric glass transition temperature T_g. Subsequent analysis led to the conclusion that the structural arrest predicted by mode-coupling approximations is not the same as the calorimetric glass transition but rather is related to dynamic anomalies in supercooled liquids at temperatures above T_g. The application of the mode-coupling equations to supercooled liquids and the discussion of their solution is called mode-coupling theory (MCT) and has made remarkable advances the past few years [7, 8]. The two recent review articles by Götze and by Götze and Sjögren are an excellent introduction to the subject, and the reader will find most of the relevant references there [9, 10].

Since MCT makes many very interesting predictions about the behavior of certain equilibrium correlation functions and the type of singularities of certain transport coefficients and relaxation times (see Sec. II for details), experiments were performed to look for these anomalies. By means of neutron and light scattering and various spectroscopic techniques, the intermediate scattering function and the susceptibility for various systems were investigated, and several predictions of the theory were confirmed [11–18]. Whereas the earlier experiments were often able to test the predictions in only a qualita-

tive way [12–15], newer results also show an impressive quantitative agreement of experiment and theory [19–23].

Predictions of MCT have been tested and observed for a wide variety of liquids, including organic glass formers, ionic glass formers, and polymers. These systems are considerably more complex than the simple atomic liquids whose kinetic theory first led to a derivation of equations containing mode-coupling terms. This has led to the equations of MCT being regarded as a general mathematical model for nonlinear relaxation dynamics [9, 10], even for systems for which the equations have not been derived from a more microscopic theory. However, it should be kept in mind that MCT is not a universally valid theory in the sense that all supercooled liquids show the behavior predicted by the theory. Although for all dense liquids the equations of motion for the correlators presumably contain mode-coupling terms, for some systems these terms might be so small compared with other terms that they do not lead to any measurable effect. So far no criterion is known to decide *a priori* whether or not a system should show the phenomena predicted by MCT, and many systems do not seem to behave according to the theory. Thus, adding to our understanding of the kind of systems to which MCT applies and the extent to which it does so is of great importance.

MCT has not only been tested in real experiments but has also been used to interpret the results of computer simulation studies of supercooled liquids [24–30]. As with real experiments, some simulations seem to confirm certain predictions of the theory and others do not. One problem with computer simulations is that simulated supercooled liquids are likely not to be thoroughly equilibrated if the runs are not much longer than the long relaxation times that prevail at such low temperatures. This of course can be a big disadvantage for testing an equilibrium theory. Another handicap of computer simulations is that the time range that a simulation can cover is usually only two or three orders of magnitude larger than typical microscopic times, whereas some of the tests of the predictions of MCT require time windows which are considerably larger. However, these kinds of "computer experiments" have a big advantage over real experiments: they allow the measurement of many different correlation functions, some of which are almost impossible to measure in real experiments, at the *same* time and therefore for the same thermodynamic state. This makes it possible to perform stringent tests of certain predictions of MCT. These tests would be very difficult for real experiments since their outcome is very sensitive to the thermodynamic state.

The system we deal with in this paper is a kinetic lattice gas with particles having a hard core and other short-range interactions. Lattice gases, originally proposed to study hydrodynamic phenomena [31], have found widespread use in studying many kinds of dynamical behavior. A representative list of these topics can be found in [32]. The main reason for this popularity is that their implementation on a computer can be made very efficient, thus allowing the investigation of time scales that are considerably longer than those accessible for more frequently studied systems, such as Lennard-Jones particles or soft spheres. Thus with this model, it will be possible to make tests of MCT that are probably more sensitive than similar tests performed on more commonly studied systems since one can make longer runs to equilibrate and cover larger time windows for the correlation functions. In addition it can be hoped that, because of the simple nature of lattice-gas systems, it will also be possible to make progress on the analytical side so that the phenomenon of the MCT singularity can be better understood [33]. Note that, although lattice-gas models for supercooled liquids have been investigated before [34, 35], no comparison with MCT predictions have been made so far. Since MCT has become regarded as a general model for nonlinear relaxation, it is not unreasonable to test it for kinetic lattice gases.

In the next section we summarize those formulas of MCT that are important for this work. Section III introduces the model and gives the details of the simulations. Section IV is then devoted to the presentation and discussion of the results, and in Sec. V we give a summary and draw our conclusions.

II. MODE-COUPLING THEORY

Mode-coupling theory, as formulated in the review articles of Götze [9] and Götze and Sjögren [10], is a very general theory that can explain and make predictions about a wide variety of types of relaxation behavior of supercooled liquids. In this section, and in most of the text of this paper, we shall be concerned with the mode coupling theory of what is called a B transition at an A_2 singularity (or A_2 fold). Other types of transitions or singularities can also arise and lead to different kinds of relaxation behavior near T_c. Moreover, we consider only the case in which coupling of particle densities to currents, which leads to phonon assisted transport, is completely neglected. When this coupling is included in the theory, the dynamical singularity is avoided, the mode coupling equations predict ergodic behavior even below T_c, and the behavior of the correlation functions near T_c may be either slightly or significantly changed, depending on the strength of the coupling. Unless otherwise noted, whenever MCT is referred to in the following discussion, this particular special case is what is meant. It is in fact the version of the theory that has been most well developed and most extensively compared to experiment.

In the following we compile those formulas of MCT which are relevant for our work and some of their implications. Their derivation can be found in the original papers or in the review articles by Götze and by Götze and Sjögren [9, 10].

Consider a system consisting of N classical, identical particles. The central focus of MCT is the behavior of the equilibrium correlation functions $\Phi_q(t)$ obtained by normalizing the intermediate scattering function $F(\mathbf{q}, t)$ by the static structure factor S_q:

$$\Phi_q(t) = \langle \rho_q(t)\rho_{-q}(0)\rangle / S_q \quad . \tag{1}$$

Also the dynamic structure factor $S(\mathbf{q}, \omega)$, given by the time Fourier transform of $F(\mathbf{q}, t)$, plays an important

role in the theory. The fluctuation-dissipation theorem connects $\omega S(\mathbf{q},\omega)$ with the imaginary part of the dynamic susceptibility $\chi''(\mathbf{q},\omega)$, and in the literature of MCT these two quantities are often set equal to one another, i.e., $\chi''(\mathbf{q},\omega)=\omega S(\mathbf{q},\omega)$.

Equations of motion for the correlator $\Phi_q(t)$ lead to the following expression for its Laplace transform $\Phi_q(z)=i\int_0^\infty \exp(izt)\Phi_q(t)$ (for $\mathrm{Im}z>0$):

$$\Phi_q(z)=-1/\{z-\Omega_q^2/[z+M_q(z)]\} \quad . \tag{2}$$

Here $\Omega_q=(q^2v^2/S_q)^{1/2}$ is a characteristic frequency, and $v=\sqrt{k_BT/m}$ is the thermal velocity. M_q is a relaxation kernel, and in the simplest form of MCT (i.e., when the couplings to currents and to fluctuations of the energy are neglected), it is approximated by the functional

$$M_q(t)=\sum_{q_1}V^{(1)}(q,q_1)\Phi_{q_1}(t) +\frac{1}{2}\sum_{q_1,q_2}V^{(2)}(q,q_1,q_2)\Phi_{q_1}(t)\Phi_{q_2}(t)+\cdots \quad . \tag{3}$$

Vertices $V^{(j)}$ are non-negative and can, under certain approximations, be expressed as functions of S_q and are therefore dependent on temperature (or density).

When Eqs. (2) and (3) are solved for certain choices of the vertices $V^{(j)}$, it is found that under certain conditions the correlation functions do not decay to zero in the limit of long times, which suggests that the dynamics of the system is not ergodic. Let us consider the situation in which the density of the system is fixed and the temperature T is the only thermodynamic variable required to specify the state of the system. The states for which the correlation functions decay to zero are interpreted as liquid states and the highest temperature at which the functions do not decay to zero is denoted T_c. The transition from ergodic behavior (above T_c) to nonergodic behavior (below T_c) is the important dynamical singularity predicted by MCT. In discussions of MCT, the scaled temperature difference from the transition temperature is denoted by $\epsilon\equiv(T_c-T)/T_c$, and MCT also introduces a so-called exponent parameter λ, which is system dependent and satisfies $0<\lambda<1$. The theory makes detailed predictions about how the correlation functions behave as a function of time t, ϵ, and λ, for small values of ϵ, i.e., for states near the transition temperature.

Furthermore, MCT predicts not only that the above mentioned correlators Φ_q behave in the way explained below, but also that all other correlators Φ_{XY} between quantities X and Y that have a nonzero overlap with density fluctuations (i.e., $\langle\rho_qX\rangle\neq0$ and $\langle\rho_qY\rangle\neq0$) behave in the same way. In this section we will therefore drop the subscript $\mathbf{q}$ from all quantities, and it is understood that the quoted results apply for all correlators Φ_{XY} where X and Y satisfy the above-mentioned conditions. However, here and throughout the paper we will still use the notation as if $X=Y=\rho_q$, e.g., we will still denote the space-time Fourier transform of $\Phi_{XY}(\mathbf{r},t)$ by $S(\mathbf{q},\omega)$ and will call it the dynamic structure factor.

Most of the predictions MCT makes fall into two categories: statements about the α relaxation and statements about the β relaxation. Many of these predictions can be stated most easily in terms of the imaginary part of the dynamic susceptibility $\chi''(\mathbf{q},\omega)$. Note that all of the following formulas are considered to be valid only in the limit $|\epsilon|\to0$ since the dynamical equations for the correlators were solved only in this limit.

A. α relaxation

The α relaxation governs the long-time behavior of the correlators and is signaled by a peak at low frequencies in $\chi''(\omega)$. In spectroscopic experiments it is observed that the position $\omega_{\max}$ of this peak moves rapidly towards smaller frequencies as the temperature is lowered, showing the divergence of the corresponding relaxation times. MCT makes the following predictions:

For $T>T_c$ ($\epsilon<0$) the frequency $\omega_{\max}$ varies critically with temperature, i.e.,

$$\omega_{\max}\propto|\epsilon|^\gamma \quad , \tag{4}$$

where exponent γ is given by

$$\gamma=\frac{1}{2a}+\frac{1}{2b} \tag{5}$$

and a and b are the (unique) solutions of the equations

$$\Gamma(1-a)^2/\Gamma(1-2a)=\Gamma(1+b)^2/\Gamma(1+2b)=\lambda \quad . \tag{6}$$

Here $\Gamma(x)$ stands for the Γ function. Since λ depends on the system, a and b, and therefore also γ, are not universal. In addition it can be shown that $0<a<1/2$ and $b>0$ hold and therefore $\gamma>1$.

The critical behavior of $\omega_{\max}$ leads to a similar behavior for the diffusion constant D. Thus in the vicinity of T_c one expects

$$D\propto|\epsilon|^\gamma, \qquad \epsilon<0 \quad , \tag{7}$$

with the same value of γ as appears in Eq. (4).

The shape of the α peak for a given system is predicted by MCT to be independent of temperature in the sense that by appropriate scaling of time, which corresponds to a shift of the curves $\chi''(\omega)$ parallel to the frequency axis in a $\log\omega$ plot, α peaks corresponding to different temperatures can be made to collapse onto a single master curve. This feature is called the time-temperature superposition principle.

Calculations on simple model mode-coupling equations have shown that the low-frequency part of this master curve can be well fitted by the time Fourier transform of a Kohlrausch-Williams-Watts (KWW) law. This means that in the time domain the long-time behavior of the correlator $\Phi(t)$ can be fitted very well by the KWW law, i.e.,

$$\Phi(t)\cong A\exp[-(t/\tau)^\beta], \qquad 0<\beta\leq1 \quad . \tag{8}$$

Note that the time-temperature superposition principle implies that the KWW exponent β is independent of temperature and that the main temperature dependence of

$\Phi(t)$ is in the time scale $\tau(T)$. In general the value of β will depend on the quantity studied; i.e., different correlators will have different values of β. For $\beta < 1$ the width of the α peak is broadened as compared with the Debye law ($\beta = 1$), a property called α stretching. A value of β of 0.5 leads, for example, to an α peak with a half-width of about two decades in a plot of $\chi''(\omega)$ versus $\log\omega$, whereas a Debye peak has only a width of 1.14 decades. Hence the former peak is almost one order of magnitude broader than the latter one.

For the high-frequency wing of the α peak, systematic deviations from the KWW law are predicted. This range of the spectrum coincides with the low-frequency part of the β relaxation, which we will discuss now.

B. β relaxation

The β-relaxation process occurs in the time range between microscopic times and the large times for which the α process becomes relevant. In this time interval the solutions of Eqs. (2) and (3) are of the form

$$\Phi(t) = f + h\sqrt{|\epsilon|}g_{\pm}(\hat{t}) \quad \text{with} \quad \hat{t} = t|\epsilon|^{1/2a}/t_0 \quad . \tag{9}$$

Here h is an amplitude factor that is independent of temperature, but in general dependent on the quantity studied, t_0 is a microscopic time, and $\pm$ refer to $\epsilon \gtrless 0$, respectively. The constant f, the nonergodicity parameter, depends weakly on temperature and also on the quantity studied. For the case $X = Y = \rho_q$, f is the Debye-Waller factor, while for the case $X = Y = \rho_q^s$, where ρ_q^s is the self part of the density fluctuations, f is the Lamb-Mössbauer factor. Equation (9) shows that $\Phi(t) - f$ is a product that can be separated into a factor $g_{\pm}$ that only depends on the rescaled time $\hat{t}$ and a time-independent factor that depends on temperature and in general on the quantity under investigation. The function $g_{\pm}(\hat{t})$ has no explicit temperature dependence and for $\hat{t} \ll 1$ is given by a power law

$$g_{\pm}(\hat{t}) \propto \hat{t}^{-a} \quad . \tag{10}$$

For $\hat{t} \gg 1$, one finds on the glass side (i.e., $\epsilon > 0$)

$$g_{+}(\hat{t}) \to 1/\sqrt{1-\lambda} \tag{11}$$

and on the liquid side ($\epsilon < 0$)

$$g_{-}(\hat{t}) = -B\hat{t}^{b} \qquad \text{with} \quad B > 0. \tag{12}$$

Equation (11) holds for all $\hat{t} \gg 1$, whereas Eq. (12) is valid only for those times for which $h\sqrt{|\epsilon|}g_{-}(\hat{t})$ is small compared to one. Note that exponents a and b appearing in Eqs. (10) and (12) are the same quantities that appeared in Eq. (5), which shows how closely, from the point of view of MCT, the α and β relaxation are tied together.

The power law in Eq. (12) is called the von Schweidler law. Note that exponent b and exponent β in the KWW law are not related to each other. Therefore the von Schweidler law should not be considered as a short-time expansion of the KWW law.

From Eqs. (9) and (11) we see that the asymptotic value of $\Phi(t)$ for long times will grow like $\sqrt{\epsilon}$ when the temperature is lowered below T_c. Thus the theory predicts an anomalous increase of f over its regular temperature dependence for $\epsilon > 0$.

Both power laws in (10) and (12) will give rise to a power law in the imaginary part of the susceptibility as well, but now with exponents a and $-b$, respectively. Therefore there will be a minimum in $\chi''(\omega)$ whose position and value we denote by $\omega_{\min}$ and $\chi''_{\min}$, respectively. MCT makes the prediction that both quantities vary critically as well, i.e.,

$$\omega_{\min} \propto |\epsilon|^{1/2a} \quad , \tag{13}$$

$$\chi''_{\min} \propto |\epsilon|^{1/2} \quad . \tag{14}$$

Because $g_{\pm}$ in Eq. (9) is independent of the quantity studied, the theory implies that the exponents a and $-b$ and the frequency $\omega_{\min}$ are *independent* of the quantity under investigation.

III. MODEL

In this section we introduce our model and give some of the technical details about our simulation.

The model is a kinetic lattice gas in which each particle has a discrete set of possible positions on the vertices of a simple cubic lattice and has six possible values of the momentum, all of the same magnitude and pointing along the $\pm x$, $\pm y$, and $\pm z$ directions. Moreover, in this model, time is also regarded as a discrete variable. This complete discretization of position, momentum, and time can lead to enormous computational efficiency. The model can be regarded as a type of "cellular automaton" model. A major goal of this work is to combine the efficiency that cellular automata calculations can achieve with a model that contains some of the important physical features of real glass forming liquids.

To mimic the strong short-ranged repulsive forces of real liquids, we chose to make the interparticle potential infinite if two particles are on the same lattice site. To give the system thermodynamic properties that are nontrivially dependent on temperature, we included some additional short-ranged attractions and repulsions of finite strength. To prevent crystallization at low temperatures we decided to have a mixture of particles: N_A of type A and $N_B < N_A$ of type B. To simplify the model, the interaction between particles of the same kind was chosen to be the same for both species. The interaction between like particles was chosen to be

$$V_{AA}(r) = V_{BB}(r) = \begin{cases} \infty, & r = 0,1 \\ 1, & r = \sqrt{2} \\ 0, & r > \sqrt{2} \end{cases} \quad , \tag{15a}$$

and that for unlike particles was chosen to be

$$V_{AB}(r) = V_{BA}(r) = \begin{cases} \infty, & r = 0,1 \\ -1, & r = \sqrt{2} \\ 1, & r = \sqrt{3} \\ 0, & r > \sqrt{3} \end{cases} \quad . \tag{15b}$$

Here the unit of length is the lattice spacing and the units of energy is $V_{AA}(\sqrt{2})$.

This choice of $V_{AB}(r)$ prevents the formation of large three-dimensional crystals at low temperatures if the concentrations of A and B particles are significantly different. However, two-dimensional crystallites consisting of planar arrays of particles with each A particle having four B particles as neighbors at a distance of $\sqrt{2}$ and each B particle having four A particles at that distance, are still possible. At low density the ground state of the system will consist of many such crystallites arranged in a random way. The size of these crystallites is determined by the excess of the number of A particles over the number of B particles as the former will form the boundary of the crystallites. Thus at low density the ground-state energy per particle will be $e_{\min} = -4N_B/(N_A + N_B)$ since in this case every B particle is surrounded in an optimal way by four particles of type A. Note that the ground state is highly degenerate as each crystallite can be moved around without changing the energy of the system as long it does not start to interact with another crystallite.

The state of a system can be regarded as a point in a discrete phase space. In the following discussion we will denote the general phase point by lower case letters, e.g., a, b.

The energy of a phase point $E(a)$ is simply chosen to be the sum of the potential energies of interaction between each pair of particles. Kinetic energy is ignored because we assume that each of the six allowed values of momentum has the same magnitude and hence the same value of the kinetic energy. Thus, in this model the kinetic energy is a constant and can be absorbed into the zero of energy. At equilibrium, the probability that the system is in a state a is

$$P_a^{\text{eq}} = \exp[-\beta E(a)]/Q(\beta) \quad , \tag{16}$$

where

$$Q(\beta) = \sum_b \exp[-\beta E(b)] \quad , \tag{17}$$

$\beta = 1/k_B T$, T is the temperature of the system, and k_B is Boltzmann's constant. (P^{eq} and Q also depend, of course, on N_A, N_B, and the number of lattice sites.)

The dynamics of the model must be characterized by a set of rules for determining how the discrete state of the system changes from one discrete time to another. The real Hamiltonian dynamics in a continuous-phase-space description of a fluid has a number of important properties: It is deterministic. It is time-reversal invariant. Both momentum and energy are conserved. The interactions are short ranged. The canonical distribution function is stationary under the Hamiltonian dynamics.

While cellular automata models can be constructed that have all these properties, for very simple forms of the energy or Hamiltonian we were not able to construct a model that had all these properties for the type of interactions described above. (In particular, the hard-core part of the interaction proved to be a stumbling block.) Instead we constructed a model that was consistent with the complicated interactions and that preserved several but not all of these dynamical features.

The motion is a Markov process governed by a set of transition probabilities W_{ab} defined so that W_{ab} is the probability that the system will be in state a at time step $n+1$ given that it is in state b at time step n. The transition probabilities are all non-negative and are normalized in the usual way,

$$\sum_a W_{ab} = 1 \quad \text{for all } b \quad . \tag{18}$$

For any state a, the corresponding time-reversed state $T(a)$ will be defined as the state in which the particles have the same positions as in a but have momenta that are the negative of the momenta in a. Thus, T is a one-to-one mapping of phase space onto itself. Time-reversal symmetry of the model involves two conditions: one for the equilibrium distribution and one for the dynamics. We demand that the equilibrium distribution satisfy

$$P_a^{\text{eq}} = P_{T(a)}^{\text{eq}} \quad \text{for all } a.$$

This is clearly satisfied by Eq. (16). We also demand the following condition on the transition probabilities:

$$W_{ab} P_b^{\text{eq}} = W_{T(b)T(a)} P_{T(a)}^{\text{eq}} \quad \text{for all } a \text{ and } b \quad . \tag{19}$$

This is a generalization of the microscopic reversibility condition of mechanics. It will play the same role in the current theory as the detailed balance condition plays in a discussion of Monte Carlo simulation of Markov processes.

From the generalized microscopic reversibility relationship, Eq. (19), and the normalization condition, Eq. (18), it can easily be shown that

$$\sum_b W_{ab} P_b^{\text{eq}} = P_a^{\text{eq}} \quad \text{for all } a \quad . \tag{20}$$

This implies that the dynamics of the model when applied to a canonical distribution of states preserves the canonical distribution, or, in the language of the theory of Markov processes, the canonical distribution is a stationary distribution for the process. We shall refer to Eq. (20) as the stationarity condition.

The transition probabilities were constructed to satisfy Eqs. (18), (19), and hence (20). The resulting model could be regarded as a generalization of traditional Monte Carlo models by the introduction of momentum degrees of freedom. Alternatively, it could be regarded as a simplification of continuous mechanics to a discrete process that preserves some of the important features of real dynamics.

The following is a description of the algorithm for the process: In each time step we randomly pick one particle (say particle i) and decide randomly whether to try to move it or to try to make it suffer a binary collision. The probability associated with each of these two possibilities is 0.5. If we decide to try a move we move particle i in the direction of its velocity by one lattice spacing. As in the standard Metropolis algorithm, if this move would lead

to a decrease in the potential energy of the system, then the move is definitely accepted. If the move would lead to an increase in the potential energy, then the move is accepted with probability $\exp(-\Delta E/k_BT)$, where ΔE is the potential-energy increase. In either case, if the move is accepted, the final state of the system is the state with particle i moved and with its momentum unchanged and all other particles unaffected. If the move is rejected, then the final state of the system is one in which particle i is unmoved but its velocity is the negative of what it was in the initial state and all other particles are unaffected. If we decide to try to make it suffer a binary collision, we count the number of particles that are second, third, or fourth nearest neighbors of particle i. If we find none, then no collision occurs and the final state is the same as the initial state. If we find at least one neighbor we choose one of them at random (say particle j). If the following three conditions are met—(1) particle j is a second nearest neighbor of particle i, (2) the velocities of the two particles point in opposite direction, and (3) the dot product of the relative position $\mathbf{r}_{ij}$ and relative velocity $\mathbf{v}_{ij}$ is negative—then both velocities are rotated by 90° in the plane spanned by $\mathbf{r}_{ij}$ and $\mathbf{v}_{ij}$ such that both velocities point away from the other particle. It is easy to see that this rotation is unique. We call this a "center-edge" collision because particle j is on an edge of a cube centered at particle i. If one or more of the above conditions are violated, the velocities of particles i and j are interchanged. Thus, if a collision is attempted, the final state is either the same as the initial state (if the particle chosen for the collision has no second, third, or fourth neighbors, or if the two particles in the collision have the same momentum in the initial state) or it differs from the initial state only in the velocities of the two particles i and j, all the positions of all the particles and the velocities of all the other particles being the same as in the initial state.

This algorithm has four important features that are consistent with normal dynamics in fluids. (1) A particle can move only in the direction of its momentum. (2) Collisions between pairs of particles can take place only if they are a short distance apart. (3) The collisions conserve momentum. (4) The transition probabilities are consistent with the generalized microscopic reversibility condition, Eq. (19), and hence the stationarity condition, Eq. (20). The first three features are easily demonstrated. Demonstration of the fourth is straightforward but tedious.

This algorithm also has some unphysical features (besides the discretization of space, momentum, and time). (1) The dynamics does not conserve momentum, because an unsuccessful move leads to a reversal of the momentum of one particle. Such velocity reversals (or a similar feature) must be incorporated in the model to ensure satisfaction of the generalized microscopic reversibility condition. We tried to construct a model that conserved momentum completely and that had hard-core interactions, but we were unsuccessful. We strongly suspect, but we cannot prove, that it is impossible to construct a model, of the type discussed here, with both hard-core interactions and momentum conservation. (2) A binary collision between two particles is possible even if they are moving away from one another, i.e., if the dot product of their relative velocity and relative position is positive. We were not successful in devising a more physically reasonable binary collision algorithm that was consistent with generalized microscopic reversibility. (3) The dynamics does not conserve energy. Under conditions in which the motion is ergodic, long-time averages of properties correspond to canonical, rather than microcanonical, ensemble averages.

Some of the details of the dynamics were chosen to avoid the creation of unphysical constants of motion. The physical motivation for having binary collisions in the model is clear, but we note that in the absence of the binary collisions, the momentum reversals associated with the single-particle attempted moves would not be adequate to equilibrate the system. In particular, each particle would be confined to the line defined by its initial position and the direction of its initial velocity. The center-edge collisions were introduced for a similar reason. If all binary collisions merely interchanged the velocities of the two particles, there would be six macroscopic conserved quantities, namely the total number of particles moving in each of the six directions would be conserved. Even introduction of the velocity reversals would still leave three conserved quantities, the number of particles moving in the $\pm x$, $\pm y$, and $\pm z$ directions.

We performed calculations using this model to obtain equilibrium thermodynamic and structural properties as well as equilibrium time correlation functions of interest. All simulations were performed on a cubic system of length $l = 26$ under periodic boundary conditions. The number of A particles was 560 and that of B particles was 240. The length of the runs of the simulations was between 10^5 steps per particle (SPP) for high temperatures and 10^7 SPP for low temperatures. In all cases the length of the runs during which equilibrium averages were calculated were between ten and hundred times longer than those of typical relaxation times, and the same is true for the length of our equilibration runs. This ensures that we really observe *equilibrium* quantities, a fact we consider very important for sensitive tests of MCT since this is an equilibrium theory.

Note that for a simulation with a duration of two steps per particle, each particle has on the average one opportunity either to move a distance equal to the typical interparticle distance or to suffer a velocity reversing collision because of the inability to move in the direction indicated by its velocity. For a monatomic liquid at high density, this might correspond roughly to the time for the velocity autocorrelation to change sign. This is approximately 0.2 ps for a Lennard-Jones model of argon. Thus 1 SPP is roughly equivalent to 0.1 ps. It follows that the runs we performed at the lowest temperatures correspond roughly to simulations with a duration of 1 μs. These are extremely long compared to those typically performed for molecular-dynamics simulations of supercooled liquids.

We note that the equilibrium distribution of momenta is trivial, i.e., the momentum of each particle is statistically independent of all other momenta and of the po-

sitions of all the particles. Moreover, each of the six momenta are equally likely for any particle. The distribution in configuration space is the same as that for a traditional lattice-gas model with the same potential-energy function. Thus, in principle, the equilibrium distribution in phase space could be obtained from normal Metropolis Monte Carlo calculations in configuration space and a random assignment of momenta to the particles. Since Metropolis Monte Carlo (MC) calculations are numerically considerably faster than the phase-space dynamics, we have used it for equilibration and even in the production runs. This was done in the following way. When we were computing time correlation functions we used the dynamics specified above, but after a certain number of time steps we switched to the Metropolis MC dynamics (for which no time correlation functions were computed) as it can be expected that for this kind of motion the propagation of the system in phase space is faster. Then we switched back to dynamics to continue the collection of data for the calculation of the time correlation functions. The ratio of the number of time steps used for dynamics and for Metropolis MC varied between 1 (i.e., only dynamics) and 0.01 (mainly MC) and depended on the ratio of the size of the window for which the time correlation functions were computed to the total length of the run.

From the above description of our algorithm it is clear that we need many random numbers. We generated these with a random number generator proposed recently by Marsaglia and Zaman that has been proven to be extremely reliable and very fast [36].

IV. RESULTS

In this section we present the results of our simulation. Section IV A deals with time-independent quantities such as the total energy of the system and the diffusion constant. In Sec. IV B we offer our findings about one type of correlation function and the corresponding intermediate scattering function and susceptibility. Section IV C is devoted to a second type of correlation function to investigate some predictions of MCT we were not able to test with the first type of correlation function.

A. Time-independent quantities

Figure 1 shows the total energy per particle $e_{\rm tot}$ as a function of temperature. As already mentioned in Sec. III, the ground-state configurations of the system for low densities will consist of many two-dimensional crystallites, and it is easy to show that at the density considered here the expression for the ground-state energy $e_{\rm min}$ given in Sec. III applies. In the figure, the horizontal axis is at the height of $e_{\rm min}$, which in our case is -1.2. Although the energies accessible to our simulations are still quite a bit larger than $e_{\rm min}$, it seems as if an extrapolation of $e_{\rm tot}(T)$ to lower temperatures hits the temperature axis at a nonzero value of T, which we estimate to be approximately 0.3. This value is obtained from fitting the low-temperature data with a power law

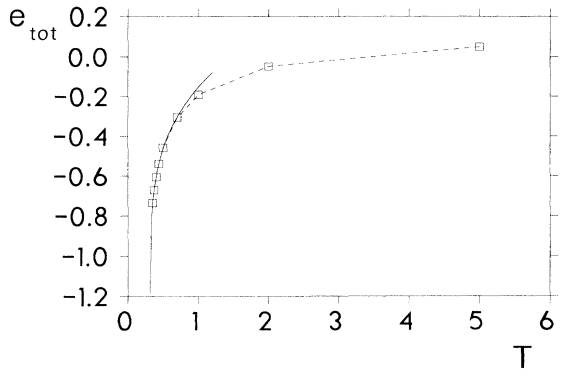

FIG. 1. Temperature dependence of $e_{\rm tot}$, the total energy per particle. The solid line is a power-law fit (see text) with exponent 0.27 and a critical temperature 0.30. The minimum energy of the system is -1.2.

$e_{\rm tot}(T) = -1.2 + A(T - T_e)^{\gamma_e}$. This fit is included in the figure as well. However, because there is no theoretical basis for this type of fitting function, the importance of the exact value of T_e should not be overemphasized since it will depend on the type of fit we have made. Thus our main point is that there exists a nonzero temperature at which the total energy might seem to behave in a singular way, although we know of course that this singularity is only an apparent one.

Figure 2 shows the self-diffusion constants D_A and D_B, for particles A and B, respectively, in an Arrhenius plot. These constants were calculated by computing the square of the net distance traveled by a particle as a function of time and by extracting the slope of the linear behavior of this function for long times. From the figure we see that the dynamical behavior of A and B particles is quite different. Although at high temperatures the values of D_A and D_B are very similar (at infinite high temperature they are exactly the same) the behavior of the two curves at low temperatures is very different. Whereas the diffusion constant for A particles levels off within the

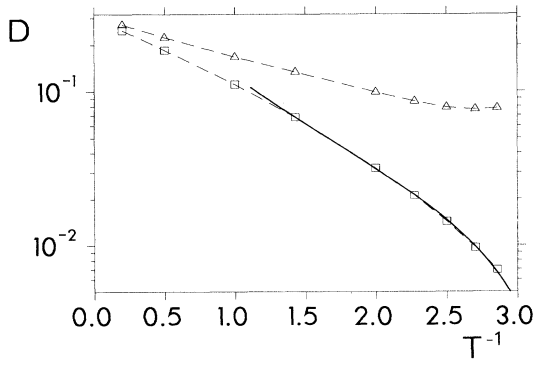

FIG. 2. Arrhenius plot of the diffusion constant D_A and D_B for A (triangles) and B particles (squares), respectively. Solid line: power-law fit with exponent $\gamma = 1.1$ and $T_c = 0.30$.

numerical accuracy, D_B decreases rapidly. We postpone for the moment the explanation for this difference until Sec. IV B 1 since we will present there further evidence which helps clarify this phenomenon. Since MCT predicts a power-law singularity for the diffusion constant in the vicinity of T_c [see Eq. (7)] we fit D_B with such a law. The best fit we found is shown in Fig. 2 as well. For this fit we have obtained a critical temperature T_c of 0.30 and a critical exponent γ of 1.1. Note that, although this value of γ is compatible with MCT (i.e., it is larger than 1.0), it is surprisingly small compared with values reported previously from other simulations [24, 25] and experiments [14–16], which are larger than 1.4. We will come back to this point again in Sec. V of this paper.

B. Time-dependent quantities

1. The van Hove function

Many of the recent computer simulations investigating dynamical properties of liquids have focused on the behavior of the van Hove function $G(\mathbf{r},t)$ defined by

$$G(\mathbf{r},t)=\frac{1}{N}\sum_{i=1}^{N}\sum_{j=1}^{N}\langle\delta(\mathbf{r}-\mathbf{r}_i(0)+\mathbf{r}_j(t))\rangle \tag{21}$$

and its self part $G_s(\mathbf{r},t)$, which is also called the tagged-particle autocorrelation function, in which only the diagonal terms $i=j$ in (21) are taken into account. $\mathbf{r}_i(t)$ is the position of particle i at time t. For isotropic systems $G(\mathbf{r},t)$ and $G_s(\mathbf{r},t)$ will depend only on the magnitude of $\mathbf{r}$, $r=|\mathbf{r}|$, thus allowing the average over the angular part of the argument to be performed. For a lattice-gas system this is not possible and we therefore introduced a quantity $G_{s1}(r,t)$:

$$G_{s1}^{(\beta)}(r,t)=\frac{1}{3N_\beta}\sum_{\alpha}\sum_{i=1}^{N_\beta}\langle\delta(r-[r_i^\alpha(t)-r_i^\alpha(0)])\rangle-\frac{1}{l}\quad , \tag{22}$$

where r_i^α is the α component of the position of particle i, $\beta\in\{A,B\}$, and the sum over i on the right-hand side goes only over particles of type β. Note that for notational convenience we will suppress the β dependence in future references to this function. Thus $G_{s1}(r,t)+1/l$ is the probability of finding at time t a particle r planes away from the plane it started in at time zero. To simplify the analysis of the data we have subtracted off the long time value $1/l$ of this probability so that $G_{s1}(r,t)$ will decay to zero.

We also defined an analogous quantity related to the total van Hove function (i.e., including the cross terms). However, the statistics for this quantity were far worse than those for G_{s1}, and since no useful tests of MCT would have been possible, the calculation was abandoned.

Figures 3 and 4 show the typical behavior of $G_{s1}(r,t)$ for A and B particles for different r. All times given in these and the subsequent figures are reported in units of SPP. The dots are the actual data points and the lines are just a guide for the eye. For clarity we will leave out the dots in most of the later graphs. For computational efficiency we calculated the correlation function for different time windows, each having a width of one to two decades in time and sampling a different part of phase space. The fact that curves stemming from different windows almost coincide at those times where the windows overlap gives an estimate for the accuracy of the data. Figure 3 shows $G_{s1}(r,t)$ for $r=0$ at all temperatures we have investigated. As for the case of the diffusion constants, we also see here that the dynamical behavior for A and B particles at low temperatures is quite different. Whereas it takes $G_{s1}(0,t)$ for the A particles about 200 SPP to decay to half of its value, it takes the same quantity for the B particles about 3000 SPP to do so. Also note the extremely slow and highly nonexponential decay of these functions at low temperatures, especially for the B particles. At the lowest temperature it takes $G_{s1}(0,t)$ 10 to 100 times longer to fall from 50% to 10% of its starting value than it takes it to fall from 100% to 50%. This shows the importance of making very long runs when the correlation times are huge and the relaxation is nonexponential. This should be taken into account when evaluating molecular-dynamics simulation data for other systems. When correlation functions decay to only half of their initial value within half of the time of the whole run, the danger of observing purely nonequilibrium ef-

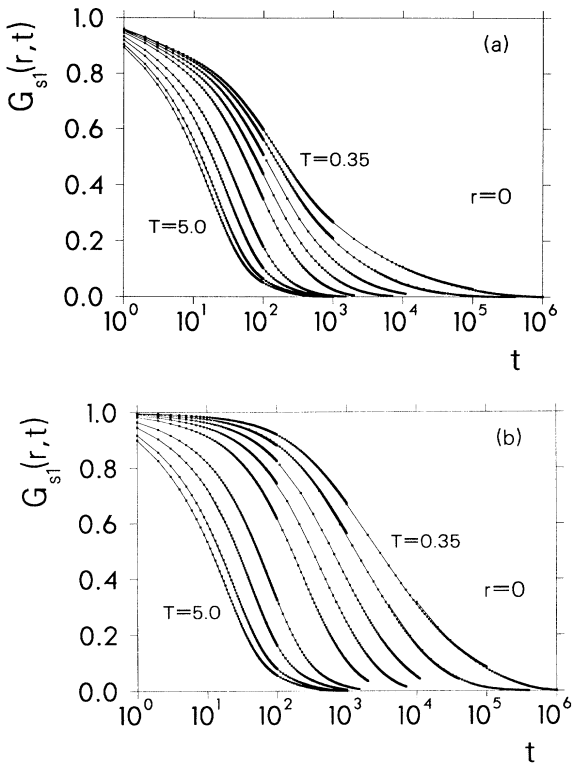

FIG. 3. Tagged-particle autocorrelation function $G_{s1}(r,t)$ for $r=0$ and temperatures 0.35, 0.37, 0.4, 0.44, 0.5, 0.7, 1.0, 2.0, 5.0 (from top to bottom). Connecting lines are only a guide to the eye. (a) A particles, (b) B particles.

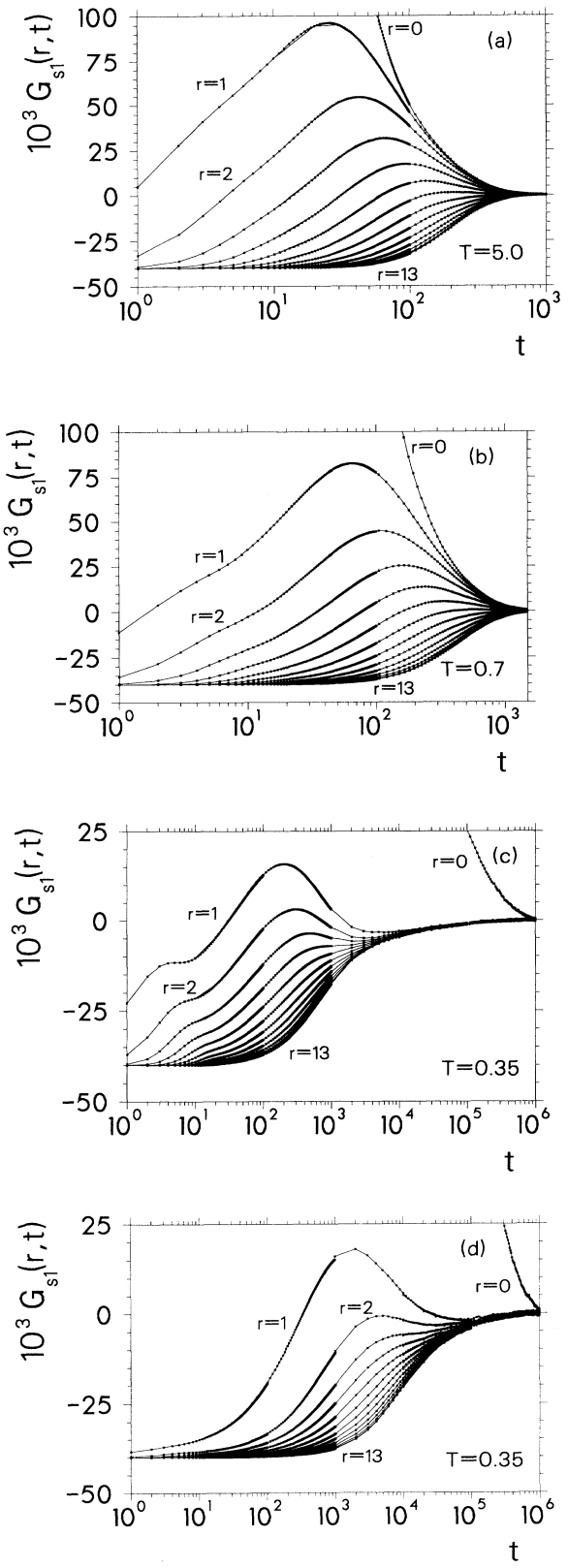

FIG. 4. Tagged-particle autocorrelation function $G_{s1}(r,t)$ for $r = 0, 1, 2, \ldots, 13$ for different temperatures. (a)–(c) A particles, (d) B particles. (a) $T = 5.0$, (b) $T = 0.7$, (c) $T = 0.35$, (d) $T = 0.35$.

fects could be very large. A more quantitative analysis of our data will be given below.

Figures 4(a)–4(c) show $G_{s1}(r,t)$ for A particles on an extended scale so that the structure of the curves for $r > 0$ becomes visible. Note that the typical values for these correlation functions are about an order of magnitude smaller than those of $G_{s1}(0,t)$. At high temperature [Fig. 4(a)] the only feature of $G_{s1}(r,t)$ for $r > 0$ is a peak whose position moves slowly to larger times for increasing r. Thus this looks like the behavior expected from a diffusive motion. Lowering the temperature to 0.7 makes the position of each of these peaks move to larger times [see Fig. 4(b)]. This is also in accordance with diffusion behavior. However, at this temperature we also can observe the appearance of a shoulder at times around 3–7 SPP. By lowering the temperature further to 0.35 [Fig. 4(c)] we see that the shoulder starts to evolve into a secondary peak.

For B particles the picture looks a bit different. Although the peak at long times is present [see Fig. 4(d)], it is shifted to larger times compared to the main peak for A particles at the same temperature. This could have been anticipated since we saw that the diffusion constant for B particles is smaller than that for A particles, thus showing that the relaxation time for B particles is larger than that for A particles. The more striking fact is that the size of the secondary peak for the B particles is so small that it is barely visible even at the lowest temperatures studied, although a careful analysis of the data has shown that it is really present. Thus it seems that at low temperature we have two different kinds of motions for the A particles: a slow one, generating the main peak, and a fast one, generating the secondary peak. For B particles only the slow motion is relevant. We think this behavior can be explained in terms of the relative abundance of A and B particles. Since we have significantly fewer B particles than A particles at low temperatures, almost all B particles will be surrounded by A particles, making their motion very difficult since they have to overcome the attractive A-B interaction trying to keep them in place. The same is true of course for those A particles which are surrounded by B particles, but since the A particles are more abundant some of them will be bound to the B particles only weakly, i.e., by only one bond, or not at all. Thus they can move around much more easily. We think that these "fast" moving particles give rise to the small secondary peak at low temperatures and are also responsible for the leveling off of the diffusion constant for the A particles at these temperatures.

Let us dwell on this a little bit more. From Fig. 2 we recognize that the diffusion constant of the A particles at low temperatures is about one-third of its value at high temperatures. Let us assume that the dynamical behavior of the fast moving A particles at low temperatures is similar to that of all the A particles at high temperatures. From this we can conclude that at low temperatures about one-third of the A particles are fast ones and two-thirds are slow ones. Another way to understand these numbers is to remember that 30% of all particles are of type B. As mentioned in Sec. III, at low temperatures the A and B particles form small crystal-

lites with a composition that is *higher* in A particles than in B particles, since the former constitute the boundary of the crystallite. It is therefore not unreasonable to find that two-thirds of the A particles are bound to crystallites and can therefore only move slowly. Further support for this point of view can be found in Fig. 3. From Fig. 3(a) (A particles) we recognize that for high temperatures $G_{s1}(0,t)$ has decayed from 1 at $t=0$ to almost zero at $t \approx 10^2$, whereas at low temperatures it has decayed only to about 0.6. Hence, for $t \geq 10^2$ the fast A particles do not contribute to $G_{s1}(0,t)$ significantly. Thus, if we assume that at low temperatures the dynamics of the slow A particles and the dynamics of the B particles are similar, we would predict that the $G_{s1}(0,t)$ for the B particles at $t \approx 10^2$ should be about $0.6/(2/3)$ and this is indeed what is found [see Fig. 3(b)]. Therefore we have evidence that, despite the fact that the diffusion constant of the A and B particles at low temperatures are very different, the dynamics of about two-thirds of the A particles is similar to the dynamics of the B particles.

This dynamical behavior of the two kinds of particles is reminiscent to the one observed in superionic glass formers. In these systems conducting particles of high mobility, which are important for the conducting modes, move in an almost rigid matrix of particles with a low mobility. The low-mobility particles are relevant for the relaxation modes. However, unlike in these kinds of materials, in our system this matrix is composed of *both* kinds of particles. Therefore both A and B particles are important for the structural relaxation and their dynamics is strongly coupled. It consequently makes sense to test MCT on correlators for A particles as well as B particles, provided one considers only correlators such as $G_{s1}(r,t)$ whose long-time behavior is governed only by the dynamics of the slow particles and provided one restricts attention to long times (or small frequencies) and fixed r (or fixed wave vector k). However, if one would investigate a correlator which measures only the behavior of the fast A particles, one would probably find a behavior similar to the conducting modes in superionic glass formers and mode-coupling theory would not be expected to apply. An example for such a correlator would be the limiting zero wave vector and zero-frequency behavior of the Fourier transform of $G_{s1}(r,t)$ for A particles, which is related to the self-diffusion coefficient of the A particles.

2. *The intermediate scattering function*

Computing the space Fourier transform of $G_{s1}(r,t)$ we find the intermediate self scattering function $F_{s1}(r,t)$:

$$F_{s1}(k,t) = -G_{s1}(0,t) - (-1)^k G_{s1}(l/2,t) + 2\sum_{r=0}^{l/2} G_{s1}(r,t)\cos(q_k r)$$

$$\text{with} \quad q_k = \frac{2\pi}{l}k \quad . \quad (23)$$

Since we have the symmetries $F_{s1}(k+l,t) = F_{s1}(k,t)$ and $F_{s1}(k,t) = F_{s1}(l-k,t)$ the intermediate scattering func-

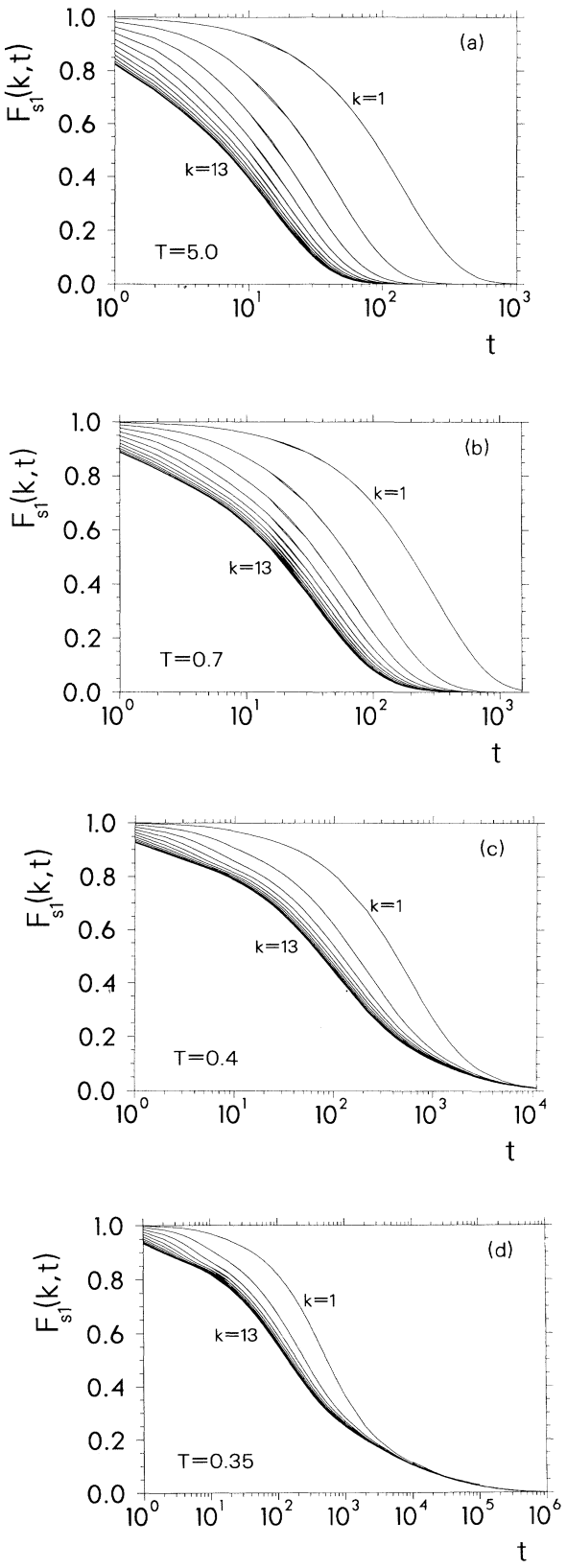

FIG. 5. Intermediate self-scattering function $F_{s1}(k,t)$ for A particles and $k = 1, 2, \ldots, 13$. (a) $T = 5.0$, (b) $T = 0.7$, (c) $T = 0.4$, (d) $T = 0.35$.

tion is completely determined when we know its value for $k = 0, \ldots, l/2$. Note that, because of the sum rule $\sum_{r=0}^{l} G_{s1}(r,t) = 0$, we have $F_{s1}(0,t) = 0$ for all times.

Figure 5 shows $F_{s1}(k,t)$ for the A particles for four different temperatures. We see that for all temperatures $F_{s1}(k,t)$ decays more slowly the smaller k is. For large values of k the curves seem to approach a master curve, and this behavior is more and more pronounced the lower the temperature is. Also this collapse is more pronounced for large times, and at the lowest temperature [Fig. 5(d)] the time interval in which all curves follow the master curve stretches over more than two decades. Thus at very low temperatures (i.e., those even lower than the lowest one in this simulation) we expect that the relaxation behavior of $F_{s1}(k,t)$ is independent of k for all times. We find that this master curve is very well approximated by the spatial Fourier transform of the function given by $G_{s1}(r,t)\delta_{r,0}$ where δ is the Kronecker delta. We therefore can conclude that the main relaxation behavior of $F_{s1}(k,t)$ is given by the decay of $G_{s1}(0,t)$. Similar results hold for the B particles. MCT predicts that β relaxation is, apart from an amplitude factor h, independent of the quantity studied [see Eq. (9)]. Thus if we assume that in our case h is not, or is only weakly, dependent on k, MCT can rationalize this kind of relaxation behavior for our system at intermediate times. However, MCT makes no prediction that the α relaxation should also be independent of the quantity under investigation, and therefore our finding is surprising, although not in contradiction with the theory.

Figure 6 shows $F_{s1}(k,t)$ for $k = 1$ and 13 for the A particles at all temperatures we investigated. Although both sets of curves show a dependence on temperature, the one for the large value of k is much stronger. Of course this is just another manifestation of the previously discussed result that for low temperatures curves for different values of k approach a master curve.

Figure 7 shows $F_{s1}(k,t)$ for the B particles, $k = 13$, and all the temperatures investigated. Curves for different values of k are very similar in form. We have investigated the behavior of the intermediate scattering function for a fixed temperature and different values of k and have found that at low temperatures the curves for the various k follow a master curve just as we found for the A particles. A comparison between Figs. 7 and 6(b) shows how much slower the relaxation for the B particles is at low temperatures. We also note that the shape of the curves for short times is different. For the A particles $F_{s1}(k,t)$ has an appreciable slope at short times even for the lowest temperature whereas $F_{s1}(k,t)$ for the B particles has a slope close to zero at these temperatures. This difference is consistent with the analysis offered to explain the appearance of an additional peak in $G_{s1}(r,t)$ for the A particles, namely that at low temperatures we still have a few A particles which can move around quite easily whereas almost all B particles are immobile.

Figures 6 and 7 also demonstrate that even at low temperatures the time-temperature superposition principle predicted by MCT is clearly violated since the shape of the curves at long times changes significantly as the temperature is changed. Thus it can be expected that the predictions of MCT for the properties of the α peak will not be consistent with the data.

So far we have not made any statements about the functional form of the relaxation curves. We have tried to make fits with a KWW function, but have found that this functional form does not fit the data well even for long times. Thus this is an additional discrepancy between our results and the predictions of MCT. We have also tried to fit the long-time behavior of the relaxation curves with a power law of the form $F_{s1}(k,t) = A/t^x$, but this kind

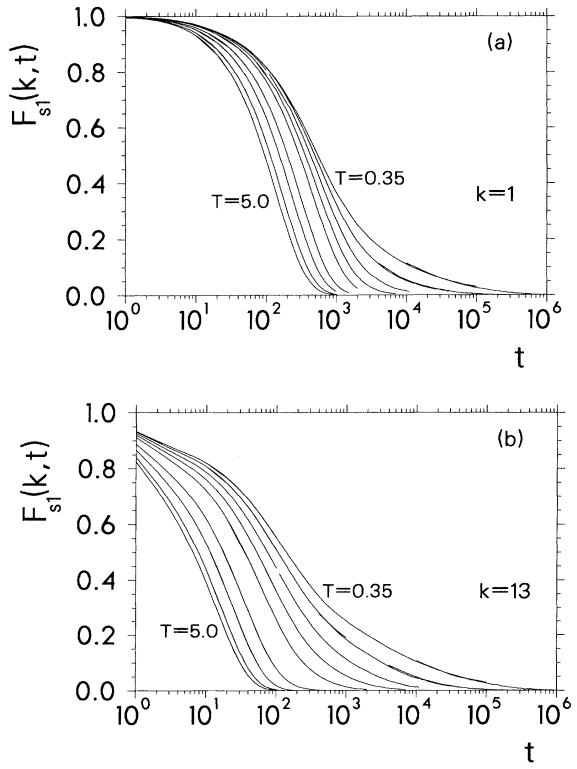

FIG. 6. Intermediate self-scattering function $F_{s1}(k,t)$ for A particles and all temperatures investigated (see Fig. 3). (a) $k = 1$, (b) $k = 13$.

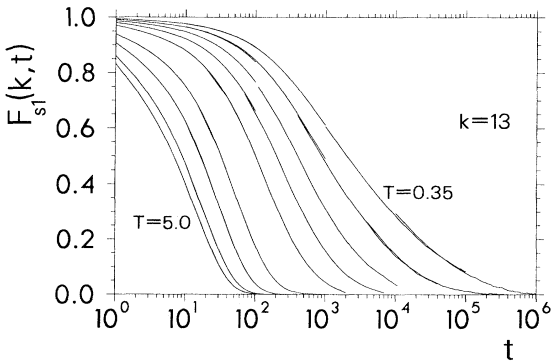

FIG. 7. Intermediate self-scattering function $F_{s1}(k,t)$ vs time for B particles for $k = 13$ and all temperatures investigated (see Fig. 3).

of fit was not convincing either. We will come back to this point later when we discuss the dynamic structure factor.

Since we were unable to fit the relaxation curves with a simple functional form, the assignment of a relaxation time $\tau(T)$ is somewhat arbitrary. Note that the usual definition for the relaxation time, the time for which the correlator has decayed to e^{-1} of its initial value, is in our case arbitrary too. This definition is only appropiate if the correlators for different temperatures can be represented by a function $C(t/\tau(T))$ with a temperature independent function C, i.e., if the time-temperature superposition principle holds. If, for example, the correlators develop a long-time tail at low temperatures as is the case here, a relaxation time defined in the abovementioned way will suggest a relaxation behavior which is too fast. We therefore have chosen to define the mean relaxation time τ to be the area under the curve. Figure 8 shows these relaxation times for the different values of k in an Arrhenius plot. For clarity we have multiplied the curves for the B particles (upper set of curves) by a factor of 10. Again we see the strong dependence of τ_A and τ_B on k for high temperatures and that this dependence almost vanishes at low temperatures. We also recognize the strong non-Arrhenius behavior of τ_A and τ_B.

Since MCT predicts a power-law divergence for the relaxation times in the vicinity of T_c [see Eq. (4)], we have tried to fit the low-temperature data with such a law. In doing this we have focused on the relaxation times for large values of k. We find that for temperatures below approximately 0.5, τ_A and τ_B can be fit very well by this type of law, and the corresponding fits are included in Fig. 8 as well. For the critical temperature T_c we find 0.327 and 0.320 for the A and B particles, respectively. The associated critical exponents γ are given by 1.99 and 2.36. These two values for T_c compare well with the T_c determined from the diffusion constant for the B particles (which was 0.30). The values for the critical exponent γ do not agree as well. However, we have noticed that, whereas T_c is not very sensitive to the kind of fit we make (e.g., what range in temperature), γ seems to be much more sensitive and is therefore much less well determined. Therefore it is difficult to decide whether the two exponents are actually different.

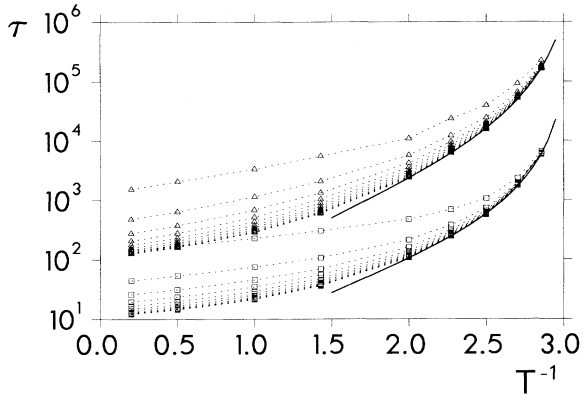

FIG. 8. Relaxation times τ_A and τ_B for A and B particles, respectively, and $k = 1, 2, \ldots, 13$. The upper set of curves are for the B particles and for clarity we plot $10 \times \tau_B$. The lower set of curves are for the A particles. Within each set, curves correspond to $k = 1, 2, \ldots, 13$ (from top to bottom). The solid curves are power-law fits to the low-temperature data. $T_c = 0.327$, $\gamma = 1.99$ for A particles and $T_c = 0.320$, $\gamma = 2.36$ for B particles.

We have also tried to fit τ_A and τ_B by the Bässler law $\tau \sim \exp(A/T^2)$ [37] and by the widely used Vogel-Fulcher law $\tau \sim \exp[A/(T - T_{VF})]$. The former did not give a satisfying fit at all. Although the latter one fit the low-temperature data with comparable quality to that of the power law, the lack of a good microscopic theory supporting such a law makes it less appealing than the power law [10].

3. *The dynamic structure factor*

Since certain types of time dependence, such as that of the von Schweidler law, are much easier to identify in the frequency domain than in the time domain we have computed the dynamic structure factor $S_{s1}(k,\omega)$, which is the cosine transform of $F_{s1}(k,t)$, for $k = 1, 4, 7, 10$, and 13 for the A particles and for $k = 13$ for the B particles. To do this we have smoothed our data a bit by means of the method of a spline under tension [38] and performed a fast Fourier transform to compute the cosine transform. Again we find that at low temperatures curves for different values of k approach a master curve. This is of course expected since the same behavior was observed in the time domain. More interesting are plots as shown in Fig. 9 where $S_{s1}(k,\omega)$ for the A particles, $k = 1$ and $k = 13$, and all the temperatures investigated are presented (corresponding plots for $k = 4$, 7, and 10 are very similar to the one for $k = 13$).

Several features can be recognized. For high temperatures and $k > 1$ $S_{s1}(k,\omega)$ goes to a constant for small ω. This is to be expected because if $F_{s1}(k,t)$ decays exponentially then $S_{s1}(k,\omega)$ is given by a Lorentzian, i.e., $S_{s1}(k,\omega) \sim 1/(1+\omega^2)$. However, if the temperature is lowered, the point where $S_{s1}(k,\omega)$ becomes independent of ω shifts to smaller and smaller frequencies, and the curves seem to approach a master curve which appears to be a straight line for $10^{-5} < \omega < 10^{-3}$, i.e., $S_{s1}(k,\omega)$ is a power law in this range of frequency. (Note that this is a different kind of master curve than the one discussed in connection with Fig. 5. There curves for different values of k at the same temperature collapsed at long times onto a master curve, whereas here curves corresponding to the same k and different temperatures show this behavior.) For intermediate ω (i.e., $10^{-2} < \omega < 10^{0}$) another power law is observed, but here the curves corresponding to different temperatures do not collapse onto a master curve. Whereas the slope of the curves is weakly dependent on temperature for $k = 1$, they seem to be independent of it for $k > 1$. Since it is easier to discuss this feature with the help of the susceptibility we will postpone this discussion to Sec. IV B 4 and focus now on the power-law behavior for small ω.

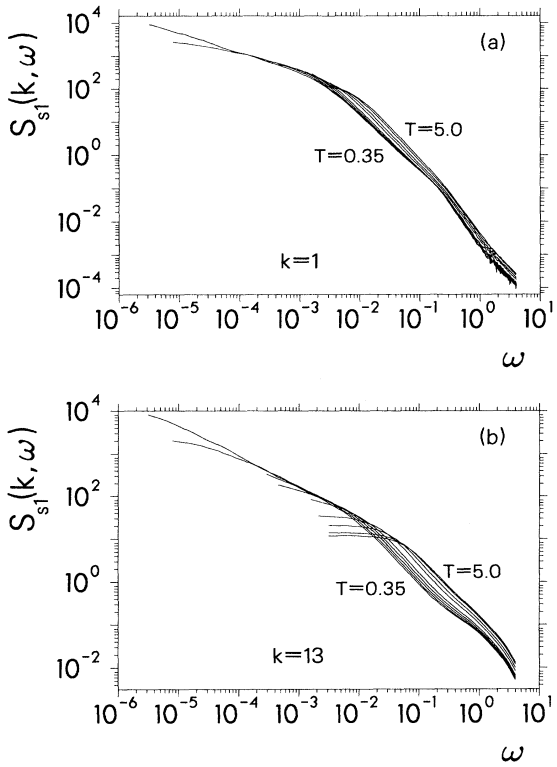

FIG. 9. Dynamic structure factor $S_{s1}(k,\omega)$ for A particles for all temperatures investigated (see Fig. 3). (a) $k = 1$, (b) $k = 13$.

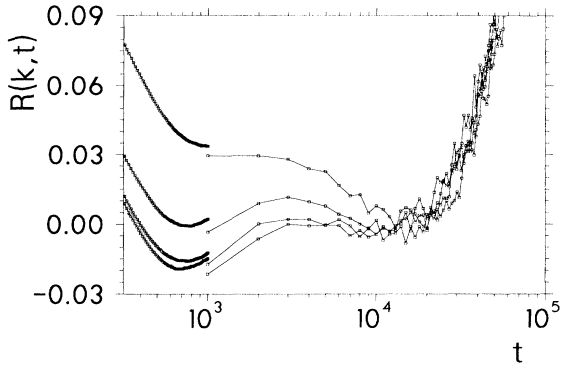

FIG. 10. Relative residuals of the power-law fit to $F_{s1}(k,t)$ for A particles for long times and $k = 4$, 7, 10, and 13 (from top to bottom). $T = 0.35$.

We have already seen that at low temperatures the long-time behavior of the relaxation curves becomes independent of k. We therefore can conclude from Fig. 9 that at these temperatures there is a frequency window at small frequencies in which all curves collapse onto each other. Since the upper boundary of this window is only relatively weakly dependent on temperature and the lower boundary shifts quickly to smaller frequencies when the temperature is lowered, the width of the window increases with decreasing temperature. As can be seen from Fig. 9(b) this width has already reached more than two decades in frequency for the lowest temperature investigated here. For the slope we obtain -0.745. This corresponds to a power law in the time domain with an exponent -0.255. The reason we were not able to fit the long-time behavior of $F_{s1}(k,t)$ with a power law is the presence of an offset P, i.e.,

$$F_{s1}(k,t) \cong P + \frac{A}{t^{\delta}} \quad \text{with} \quad \delta = 0.255 \quad , \tag{24}$$

as a nonzero P will lead to curved lines in a log$t$-logF_{s1} plot. In Fig. 10 we show the *relative* residuals $R(k,T) = [F_{s1}(k,t) - P - A/t^{\delta}]/F_{s1}(k,t)$ for $T = 0.35$ and where A is a k-independent fit parameter. That the relative residuals are so small demonstrates the numerical significance of the fit. We also can see from this plot that Eq. (24) holds within a few percent in the time range $3 \times 10^2 \leq t \leq 3 \times 10^4$. Surprisingly the fit yields a value for P of about -0.088, i.e., it is negative. This means that Eq. (24) cannot hold for arbitrarily long times since the right-hand side would become negative. We will come back to this point in the discussion.

Because the relaxation behavior for the B particles is slower than the one for the A particles, the frequency region in which the power law holds, if it exists, is at so small frequencies that it is barely visible in the frequency window accessible to our simulations. Thus no definite statement on the existence of a power law for the B particles can be made.

4. The dynamic susceptibility

Multiplying $S_{s1}(k,\omega)$ by ω yields the imaginary part $\chi''_{s1}(k,\omega)$ of the dynamic susceptibility, which is shown in Fig. 11 for the A particles, $k = 1$, 7, and 13 and all the temperatures investigated. There are two discernible features. At frequencies $\omega < 10^{-1}$, we clearly observe an α peak and we see that the two power laws mentioned in the preceding subsection correspond to the high- and low-frequency wings of the peak. In addition we see a microscopic peak at frequencies $\omega > 10^{-1}$, although at high temperatures it is not well developed since it is hidden by the α peak. Only at lower temperatures, where the α peak has moved to smaller frequencies, does the microscopic peak become readily visible. We see that, although its position is independent of temperature, it shifts to larger frequencies when k is increased, a behavior expected from the kinetic theory of fluids [3]. Also note that the form of the microscopic peak differs from the one found for example in $Ca_{0.4}K_{0.6}(NO_3)_{1.4}$ by Li *et al.* [20] in that our peak is less sharp. This might be due to the fact that our hard-core interactions lead to a strong anharmonicity and thus to a broad microscopic peak. However, Li *et al.* found for Salol a spectrum which is very similar to the one presented here [21].

From Fig. 11 we recognize that in the region of the high-frequency wing of the α peak $\chi''_{s1}(\omega)$ shows a power-law behavior. This is the corresponding power law to

the one observed for $S_{s1}(k,\omega)$ at intermediate frequencies and can be identified with the von Schweidler law predicted by MCT as part of the β relaxation. We see that for large values of k the exponent $-b$ (i.e., the slope in the curves) for this power law is independent of temperature, which is also in accordance with MCT. For b we find a value of 0.50 ± 0.04. For $k = 1$ the slopes depend weakly on temperature, but as we have already seen before, the relaxation behavior for quantities with small k do not yet fall onto the master curves for short and intermediate times at the temperatures investigated here. Thus it might be that at even lower temperatures the values of the slopes will approach approximately -0.5.

In addition to the von Schweidler law MCT also predicts a second power law in the β-relaxation regime which falls between the minimum in the susceptibility and the maximum associated with the microscopic peak [see Eq. (10)]. Since MCT connects the two exponents a and b via Eq. (6), we can conclude that a for our system would be 0.285 if MCT were correct for the system. Figure 11 shows that even at the lowest temperatures the minimum in $\chi''_{s1}(\omega)$ is not well developed yet and therefore we are not able to observe the a power law. MCT is able to explain why it is difficult to observe the a power law for the tagged-particle correlator. It can be shown that the Lamb-Mössbauer factor f_{s1} [see Eq. (9)] approaches unity for small k (see, e.g., Fig. 2 in [6]) and therefore that the observation of the power law becomes difficult [39]. This is also the reason why we do not have a well-developed minimum in $\chi''_{s1}(k,\omega)$. Thus at the moment we are not able to test the laws given in Eqs. (13) and (14) and therefore are unable to use those relations to make an independent determination of the exponent a.

Since the B particles are relaxing even slower than the A particles (Figs. 6 and 7), one expects the Lamb-Mössbauer factor for the B particles to be even larger than the one for the A particles. Consequently, the observation of the a power law in the β relaxation should be even more difficult. Also, because of the slower relaxation of the B particles, the position of the α peak is expected to be shifted to smaller frequencies relative to $\omega_{\max}$ for the A particles. This is indeed what is observed in Fig. 12 where we have plotted the susceptibility $\chi''_{s1}(13,\omega)$ for the B particles [compare with the corresponding Fig. 11(c) for the A particles]. However, we clearly see that the high frequency wing of the peak shows the von Schweidler law. Since the α peak is shifted to smaller frequencies and the microscopic peak is so much smaller than the one for the A particles, the range for which the von Schweidler law holds is quite a bit larger than the corresponding one for the A particles. Again we find that the slope of the curves, i.e., the von Schweidler exponent $-b$, is independent of temperature, and our best estimate for b is 0.73 ± 0.03. This has to be compared with the value 0.5 found for b for the A particles. This result is in contradiction to MCT since the theory predicts that for

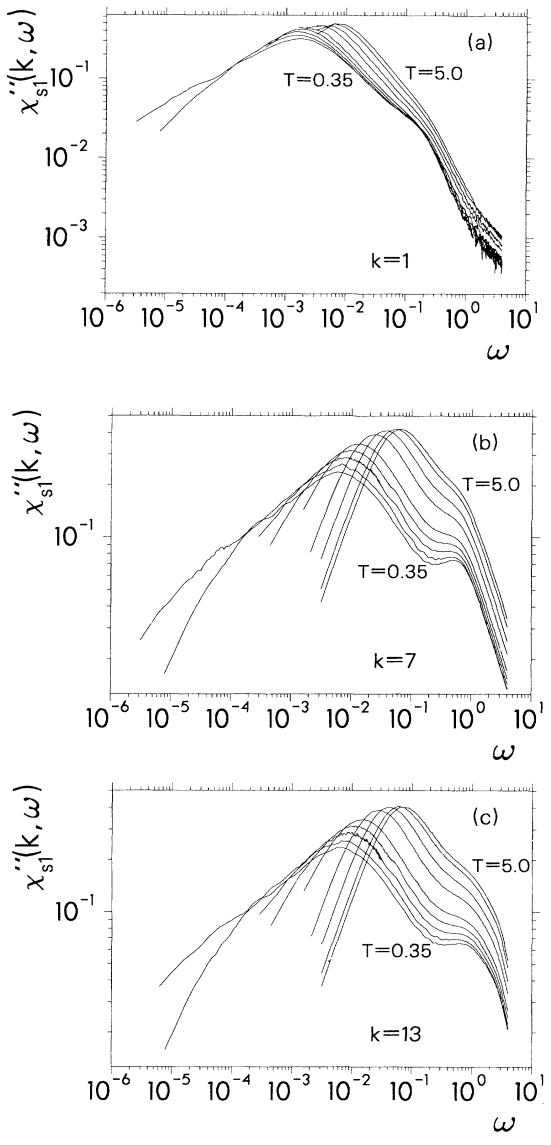

FIG. 11. Susceptibility $\chi''_{s1}(k,\omega)$ for A particles for all temperatures investigated (see Fig. 3). (a) $k = 1$, (b) $k = 7$, (c) $k = 13$.

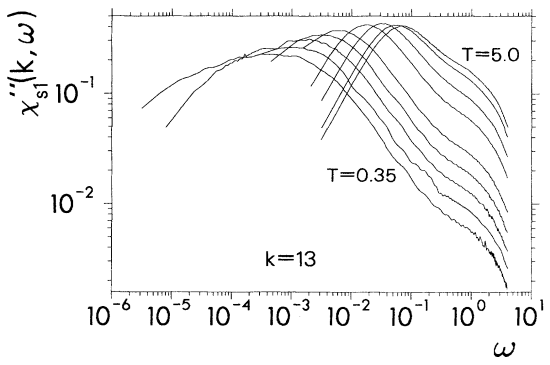

FIG. 12. Susceptibility $\chi''_{s1}(k,\omega)$ for B particles and $k = 13$ for all temperatures investigated (see Fig. 3).

a given system the values of the a and b exponents in the β relaxation regime are independent of the quantity.

The usual way to extract the Lamb-Mössbauer factor f_{s1} from the intermediate scattering function F_{s1} is to look for a plateau region and define f_{s1} to be the height of this plateau [28,29]. A second method is to use the amplitude of a KWW fit for long times as an estimate for f_{s1} [30]. In our case we cannot make use of either of these two possibilities since we neither see a plateau nor can make a KWW fit. Instead, we used another method which allows us to determine both the Lamb-Mössbauer factor and the range of validity for the von Schweidler law. We have taken the von Schweidler exponent b obtained from the fits to the susceptibility and computed the residual $Q(k,t) = F_{s1}(k,t) + B(k,T)t^b$. The von Schweidler law holds in the region where $Q(k,t)$ shows a plateau. The coefficient $B(k,T)$ can in principle be calculated from the corresponding coefficient $\tilde{B}(k,T)$ of the von Schweidler law in frequency space. However, we have noticed that we could increase the length of the plateau by regarding $B(k,T)$ as an adjustable parameter. The difference between the best value obtained for $B(k,T)$ by this method and that obtained by a direct calculation from $\tilde{B}(k,T)$ is a few percent for low temperatures and about 10% at high temperatures. Figure 13 shows the residuals for $k = 10$ and the different temperatures. Plots for $k = 7$ and 13 are qualitatively similar. Observe that the Lamb-Mössbauer factor, which is the height of the plateau, is obtained directly from this analysis. Also we can easily read off from this plot the time range for which the von Schweidler law holds since it is given by the length of the plateau. Whereas for high temperatures this range is only a few SSP ($5 \leq t \leq 10$), it extends over about 25 SSP ($15 \leq t \leq 40$) at low temperatures. Thus the time range at low temperature is comparable with the time for which the factorization property implied by Eq. (9) was found by Roux, Barrat, and Hansen to hold for a binary soft sphere system and the time for which Signorini, Barrat, and Klein found β-relaxation behavior in a simulation of a molten salt model [25,26].

In Fig. 14 we present the values for the Lamb-Mössbauer factor $f_{s1}(k,T)$ as a function of temperature

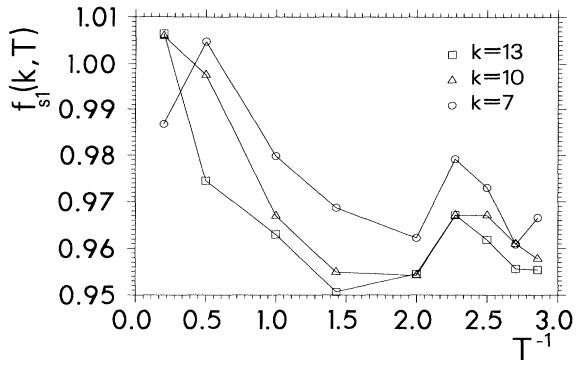

FIG. 14. Value of the nonergodicity parameter $f_{s1}(k,T)$ for $k = 7$ (circles), $k = 10$ (triangles), and $k = 13$ (squares) for A particles. We plot inverse temperature to stretch the scale at low temperatures.

for different values of k. Although the error for the data points are relatively large (as can be recognized from the scattering of the points), nevertheless we can observe two trends. First we see that the values of $f_{s1}(k,T)$ decrease with increasing k. This is in accord with MCT [6]. Second, we observe that $f_{s1}(k,T)$ increases with increasing temperature. This is in contrast with the behavior found in the experiments known to us, which show above T_c a decrease or leveling off of the nonergodicity parameter with increasing temperature (see, e.g., [13, 15, 22]). We do not know whether MCT is able to rationalize the behavior found by us since the results of the corresponding calculations for the temperature dependence of the nonergodicity parameter are usually reported only to zeroth order in ϵ. At first glance it might seem surprising that f_{s1} should increase with increasing temperature as this seems to imply that the system relaxes less the higher the temperature is. But one has to keep in mind the way we determined f_{s1}; it is just the value obtained from the extrapolation of the power-law fit to time zero and *a priori* (i.e., without the help of MCT) nothing can be said

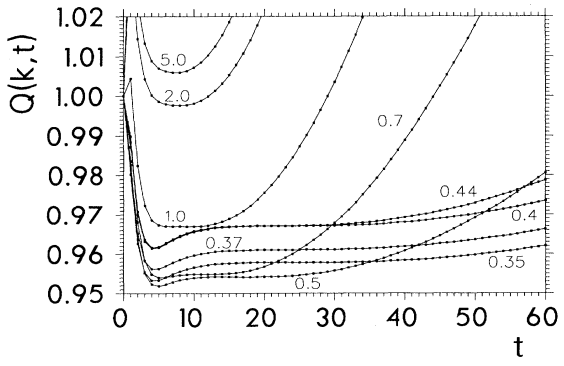

FIG. 13. Difference $Q(k,T)$ between $F_{s1}(k,t)$ for A particles and von Schweidler law Bt^b for different temperatures. $k = 10$.

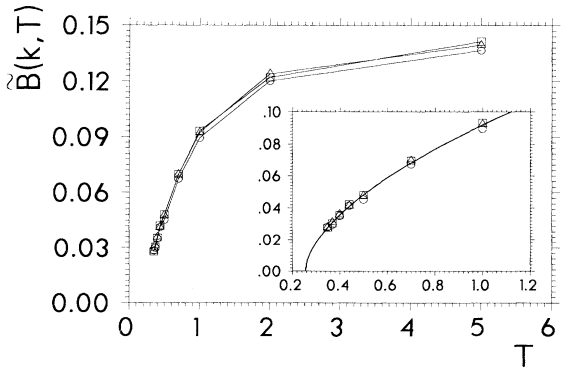

FIG. 15. Prefactor $\tilde{B}(k,T)$ of the von Schweidler law for A particles for $k = 7$ (squares), $k = 10$ (triangles), and $k = 13$ (circles). Inset: $\tilde{B}(k,T)$ at low temperatures with power-law fit (solid line). $T_c = 0.26$, $\gamma = 0.58$.

about the dependence of this value on temperature.

The fit of the von Schweidler power law to the susceptibility at different temperatures provides an additional method for extracting exponent a and the critical temperature T_c. From the Fourier transform of Eqs. (9) and (12) one easily finds that the prefactor $\tilde{B}$ of the von Schweidler law is proportional to $\epsilon^{1/2+b/2a}$. In Fig. 15 we plot $\tilde{B}$ as a function of T for $k = 7, 10, 13$. The inset shows the low-temperature part we have used to fit the power law which is included in the graph as well. For the critical temperature we obtain $T_c = 0.26$ and as critical exponent $\frac{1}{2} + \frac{b}{2a} = 0.58$. However, both quantities are subject to an error of about 10–15% as the individual data points have appreciable errors bars. The value 0.26 for T_c is about 20% lower than those obtained from the diffusion constant and from the relaxation times but taking into account the relatively large errors this is not a significant discrepancy. Using the value obtained above for b, namely 0.5, the value of a is calculated to be 3.1. Using Eq. (5) to compute a with $\gamma = 1.1$, which we found from the diffusion constant, we obtain a value for a of 5.0. Again, taking into account the error bars for a determined from the coefficient of the von Schweidler law, we do not think the discrepancy is significant, although of course neither of the two values for a is compatible with MCT, which predicts a to be less than 0.5.

We now turn our attention to the α peak. First we will discuss the time-temperature superposition principle and then comment on our findings about the α stretching.

We have already mentioned in the discussion of the intermediate scattering function that for our model we do not observe the time-temperature superposition principle predicted by MCT. To show this more clearly we plot the normalized susceptibility $\chi''_{s1}(k,\omega)$ for $k = 13$ in Fig. 16. Corresponding plots for different values of k or for the B particles look very similar. Normalization was done with respect to the position $\omega_{\max}$ and the value of $\chi''_{s1}(k,\omega)$ at $\omega = \omega_{\max}$. If the time-temperature superposition principle held, all the curves corresponding to different temperatures would collapse onto a single master curve. The graph shows that this is not the case even for temperatures as low as 0.5, a temperature which, as suggested by our results presented above, seems to be quite close to the critical temperature. However, if the previously presented analysis with the power-law behavior for small frequencies for $S_{s1}(k,\omega)$ is correct, one would expect that at very low temperatures the time-temperature superposition principle *will* hold. The high-frequency wing of the α peak corresponds to the von Schweidler law whose exponent b was found to be independent of temperature. The low-frequency wing of the peak obeys the power law at low frequencies, which we think will hold up to smaller and smaller frequencies if the temperature is lowered and whose exponent we found to be independent of temperature as well. Thus at low enough temperatures both wings of the α peak will be given by power laws with exponents independent of temperature and therefore the time-temperature superposition principle will hold. Havriliak and Negami have introduced a functional form for fitting an α peak whose wings behave asymptotically as a power law [40]. They proposed

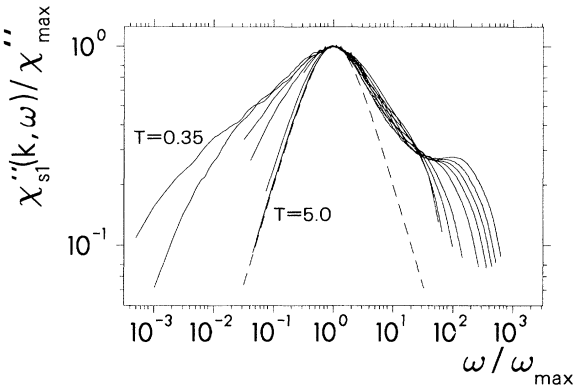

FIG. 16. Normalized susceptibility $\chi''_{s1}/\chi''_{\max}$ for A particles vs normalized frequency (see text) for $k = 13$ at all temperatures investigated (see Fig. 3). The dashed line is the predicted behavior for a Debye relaxation.

$\chi(z) \propto 1/[1 + (-iz\tau)^{a'}]^{b'}$ leading to power laws $\omega^{a'}$ and $\omega^{-a'b'}$ at low and high frequencies, respectively. We have tried this fitting function but have found that it is not able to represent the form of our curves well since the crossover region between the two power laws is too small in our case.

Although we have not been able to fit the entire α peak with a single fit function, we can still make some statements about the shape of the peak. We have included in Fig. 16 the curve that would be obtained from a pure Debye relaxation. At all temperatures we observe that the α peak is wider than the Debye peak. This is the so-called α stretching which is predicted by MCT. For our model we note that the full width at half maximum of the peaks at low temperatures is increased by about a factor of 10, and that at high temperatures the low-frequency part of the wings follow a Debye law extremely well.

To test the critical behavior given by Eq. (4) we present in Fig. 17 the position $\omega_{\max}$ of the α peak as a function of temperature for $k = 4, 7, 10$, and 13 for the A particles (upper curves) and for $k = 13$ for the B particles (lowest

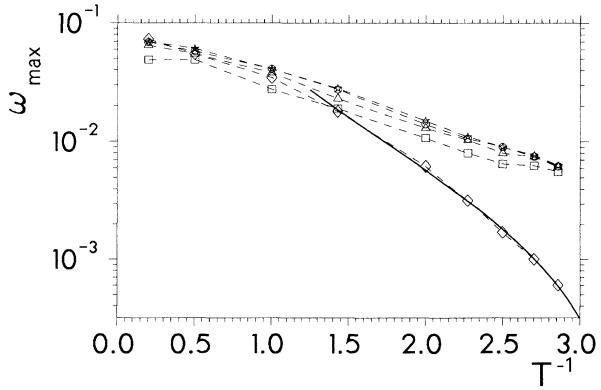

FIG. 17. Position $\omega_{\max}(k,T)$ of the α-peak for A particles and $k = 4$ (squares), $k = 7$ (triangles), $k = 10$ (circles), and $k = 13$ (stars) and B particles for $k = 13$ (diamonds). Full line: power-law fit with $T_c = 0.30$ and $\gamma = 1.7$.

curve). We see that the behavior of $\omega_{\max}$ for the A and B particles is quite different. For the latter ones we find that $\omega_{\max}$ is strongly non-Arrhenius and a power-law fit (included in the figure as well) seems to work well at low temperatures. For the critical temperature we find $T_c = 0.30 \pm 0.2$ and for the critical exponent $\gamma = 1.7 \pm 0.4$. Thus we find the behavior implied by Eq. (4). This is probably not the case for the A particles. Although the noise in the data is quite large, $\omega_{\max}$ seems to follow an Arrhenius-like behavior. A power-law fit is possible here too (T_c=0.25, γ=1.0), but taking into account the noisiness of the data, we do not think that one should give too much weight to these values.

A further quantity we investigated was $\chi''_{\max}$, the value of $\chi''_{s1}(k,\omega)$ for $\omega = \omega_{\max}$. Although to our knowledge MCT does not make any prediction about this quantity, we found that it too shows a critical behavior. Figure 18 shows $\chi''_{\max}$ for the A particles as a function of temperature for those values of k we investigated. Again it seems that there is a singularity at a nonzero temperature. Motivated by our previous results we assumed for the singularity a power-law dependence $\chi''_{\max} \propto (T - T_c)^{\gamma_A}$ and the inset shows $(\chi''_{\max})^{1/\gamma_A}$. This time the quality of the data seems to be good enough to determine the critical exponent and critical temperature quite precisely. We find $T_c = 0.324$ and $\gamma_A = 0.19$. A similar behavior is found for $\chi''_{\max}$ for the B particles for $k = 13$. We find $T_c = 0.33 \pm 0.02$ and $\gamma_B = 0.24 \pm 0.03$. So far we do not understand what the implication of this result is, but we think it to be remarkable that the T_c found in this manner is close to the critical temperatures found by other means. We are not aware of any experimental result that shows a similar behavior. Likewise, to our knowledge none of the solutions of schematic models investigated within the framework of MCT thus far shows such a behavior [9, 10]. We will comment on this further in the discussion.

C. Results for a different kind of relaxation function

Since the quantities investigated thus far have not allowed us to investigate either the high-frequency part of the β-relaxation regime or the minimum in the susceptibility we have investigated the correlation function $G_{s2}(r,t)$, which is defined as

$$G_{s2}^{(\beta)}(r,t) = \frac{1}{3N_\beta} \sum_\alpha \sum_{i=1}^{N_\beta} \langle \delta(\mathbf{r}_i(0) - \mathbf{r}_i(t) - r\hat{\mathbf{e}}_\alpha) \rangle - \frac{1}{l^3} \quad , \tag{25}$$

where $\beta \in \{\mathrm{A,B}\}$ and $\hat{\mathbf{e}}_\alpha$ stands for the unit vector of the lattice pointing in direction α. (Again we will drop in the future the superscript β in $G_{s2}^{(\beta)}$.) Thus $G_{s2}(r,t) + 1/l^3$ is the (un-normalized) probability of finding a particle at time t on one of the axes defined by the location of the particle at time zero and at a distance of r lattice spacings from its location at time zero. As in the definition of $G_{s1}(r,t)$ we subtract $1/l^3$ in (25) to make $G_{s2}(r,t)$ decay to zero in the long-time limit. Proceeding now in the same way as for $G_{s1}(r,t)$ we can define an intermediate self-scattering function $F_{s2}(k,t)$. Since we do not have a sum rule here as we did for $G_{s1}(r,t)$, the function does not vanish for $k = 0$.

Figure 19 shows $F_{s2}(k,t)$ for $k = 0, \ldots, 13$ for the A particles at $T = 0.35$. A comparison with Fig. 5(d) shows that the collapse of the curves for different values of k onto a master curve is much more pronounced than for the $F_{s1}(k,t)$ case. The time range for which this happens now extends over more than three orders of magnitude as opposed to two for $F_{s1}(k,t)$. Also at approximately 10 SPP for large enough values of k a shoulder appears. Though we will not present the plots here, we have also looked at $F_{s2}(k,t)$ for the B particles. In this case we found that the collapse onto a master curve is also more pronounced for $F_{s2}(k,t)$ than for $F_{s1}(k,t)$, but we did not see any new feature appearing in $F_{s2}(k,t)$ at short times.

In Fig. 20 we show $F_{s2}(k,t)$ for the A particles for $k = 13$ for all temperatures investigated. Now we can see how the above-mentioned shoulder is formed at low temperatures. If we compare this figure with Fig. 6(b) we recognize that at low temperatures, apart from this feature, there is no other significant difference in the relaxation behavior. In fact one finds that for times longer

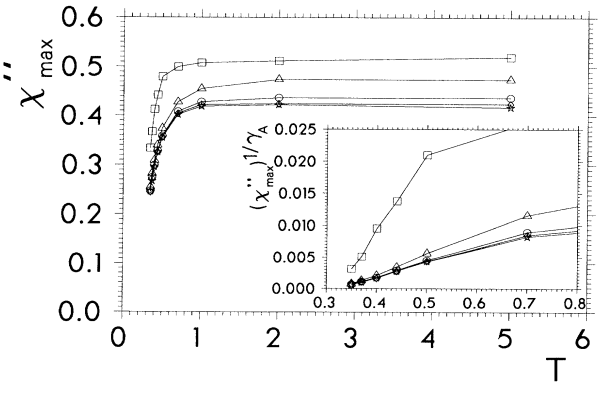

FIG. 18. Values of $\chi''_{\max}$ for A particles as a function of temperature and $k = 1$ (squares), $k = 4$ (triangles), $k = 7$ (circles), $k = 10$ (diamonds), and $k = 13$ (stars). Inset: $(\chi''_{\max})^{1/\gamma_A}$ for small temperatures. $\gamma_A = 0.19$.

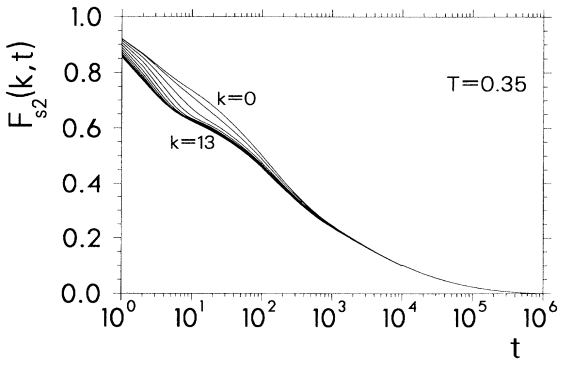

FIG. 19. Intermediate self-scattering function $F_{s2}(k,t)$ vs time for A particles and $T = 0.35$ for $k = 0, 1, 2, \ldots, 13$.

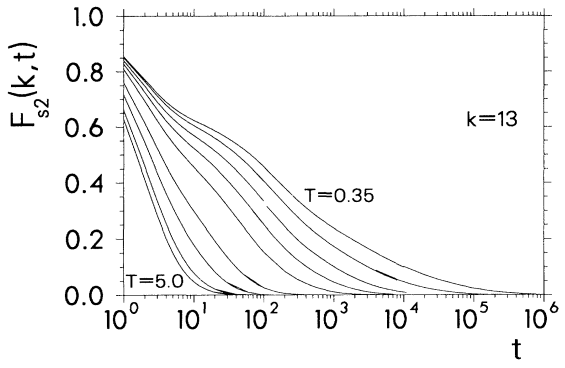

FIG. 20. Intermediate self scattering function $F_{s2}(k,t)$ vs time for A particles for $k = 13$ and all temperatures investigated (see Fig. 3).

than approximately 3×10^3 SPP the relaxation curves for F_{s1} and those for F_{s2} are the same within the numerical uncertainty. Similar plots for the B particles show that, since no shoulder appears in F_{s2} even at low temperatures, there is no significant difference in the relaxation behavior of F_{s1} and F_{s2} for B particles. As in the case for the A particles we find that for times larger than approximately 3×10^3 SPP the relaxation behavior for the two quantities coincide within the numerical uncertainty.

The presence of a shoulder in $F_{s2}(k,t)$ for the A particles is expected to lead to a well-developed minimum in the susceptibility $\chi''_{s2}(k,\omega)$. This is seen clearly in Fig. 21 where we have plotted $\chi''_{s2}(k,t)$ for $k = 13$. One can recognize that part of the wings of the minimum are more or less straight lines (i.e., power laws). MCT identifies the high- and low-frequency wings with the a power law and the von Schweidler law, respectively. Unfortunately these linear regions are very small and thus the extraction of an exponent is a bit questionable. To overcome this type of difficulty, Götze and Sjögren have proposed the formula

$$\chi''(\omega) = |\epsilon|^{1/2} \left[\tilde{A}(\omega/\omega_{\min})^a + \tilde{B}(\omega_{\min}/\omega)^b \right] \quad , \qquad (26)$$

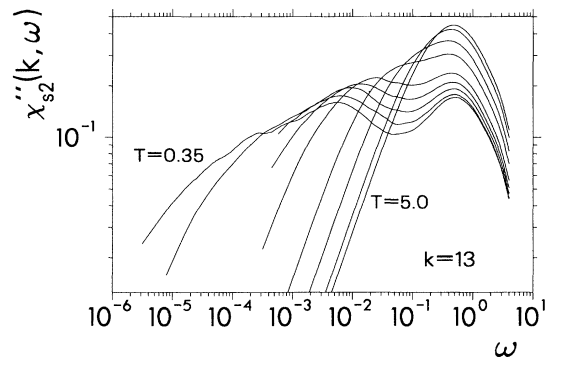

FIG. 21. Susceptibility $\chi''_{s2}(k,\omega)$ for A particles and $k = 13$ for all temperatures investigated (see Fig. 3).

which interpolates between the a power law and the von Schweidler law [8]. Since function $g_-(\hat{t})$ in Eq. (9) has no explicit temperature dependence, MCT implies that if we scale the frequency by $\omega_{\min}$, the minimum in $\chi''_{s2}(k,\omega)$, and scale $\chi''_{s2}(k,\omega)$ by $\chi''_{s2}(k,\omega_{\min})$, the curves for different temperatures should collapse onto a master curve given by the Fourier transform of $g_-(\hat{t})$. We have made such a rescaling, and in Fig. 22 we present the scaled susceptibilities for those temperatures for which we were able to identify the minimum in $\chi''_{s2}(k,\omega)$, i.e., for $T \leq 0.5$. We see that the scaling property predicted by MCT seems to hold. Also included in the figure is a fit to expression (26) (note that this function contains effectively only four fit parameters: a, b, $|\epsilon|^{1/2}\tilde{A}/\omega_{\min}^{-a}$, and $|\epsilon|^{1/2}\tilde{B}\omega_{\min}^{b}$). For the exponents a and b we find 0.56 and 0.61, respectively. These two values are not compatible with MCT as they violate Eq. (6) and the condition $a < 0.5$. A similar discrepancy has also been found in neutron scattering experiments for which other predictions of MCT seem to hold [17]. If we use Eq. (6) to connect the fit parameters a and b and redo the fit, we find $a = 0.39$ and $b = 0.99$, i.e., $\lambda = 0.503$. We have included this fit in the graph as well. Although this fit is less convincing than the first, it is not too bad a fit and it shows that the exponents can be varied by about 20% without leaving the realm of an acceptable fit. Consequently we must consider this value for b of 0.61 to compare well with 0.5, the value obtained above from χ''_{s1} for the A particles. This also suggests that the discrepancy between the b exponent values found from χ''_{s1} for the A and B particles is perhaps less severe than it seemed earlier. The value of $\lambda = 0.503$ corresponds to a value of $\gamma = 1.77$ [see Eq. (5)] which differs only slightly from the critical exponents 2.0 and 2.4 we found for the divergence of the relaxation rate for the A and B particles, respectively. However, the difference between this γ and the one obtained from the diffusion constant for the B particles (1.1) is appreciable.

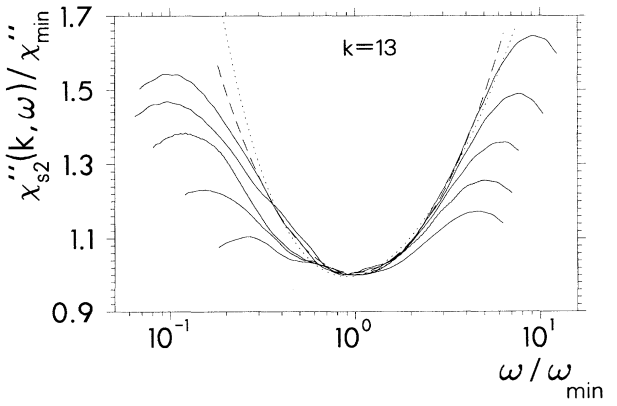

FIG. 22. Rescaled susceptibilities $\hat{\chi}''_{s2}(k,\omega)$ for $k = 13$ vs rescaled frequency. Solid curves correspond to temperatures 0.35,0.37,0.4,0.44,0.5 (top to bottom). The dashed curve is the power-law fit given in Eq. (26) with both a and b as free parameters. Connecting them via Eq. (6) yields the fit shown as the dotted curve.

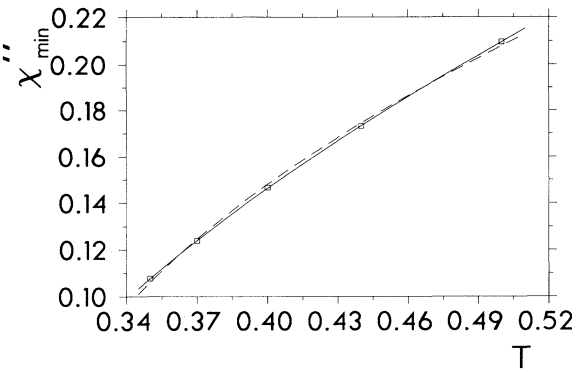

FIG. 23. $\chi''_{\min}$ for A particles (squares) as a function of T for $k = 13$. The solid line is a power-law fit with $T_c = 0.26$ and $\gamma = 0.63$. The dashed curve is fit with $T_c = 0.30$ and the MCT value $\gamma = 0.5$.

We have also computed the susceptibility χ''_{s2} for the B particles for $k = 13$ at the lowest temperature. As could be anticipated, since no shoulder appeared in F_{s2} for the B particles, no minimum in the β-relaxation region is found in χ''_{s2}. However, the range for the von Schweidler law is more than an order of magnitude in frequency, which is quite large compared with the corresponding range of validity for this law in χ''_{s1} for B particles. For the exponent we find $b = 0.55$, which compares well with the other values of b that we have extracted.

We have tried to test the critical behavior for $\omega_{\min}$ implied by Eq. (13). However, Fig. 22 shows that, due to the noise in the data, the location of the minimum $\omega_{\min}$ is not very well defined. Nevertheless, we can still see (Fig. 21) that $\omega_{\min}$ increases monotonically with temperature, but the scatter in the data prevents a power-law fit from being very informative. Therefore it is not possible to test Eq. (13). Contrary to the data of $\omega_{\min}$, the data for $\chi''_{\min}$ is sufficiently good to allow us to test Eq. (14). Figure 23 shows $\chi''_{\min}$ vs temperature. The error bars of the individual points are much smaller than the size of the symbols. Also included in the graph is the result of a power-law fit with critical exponent 0.63 and critical temperature 0.26. If one fixes the critical exponent to the MCT value of 0.5 the critical temperature increases to 0.30 but we think this fit (also included in the figure) to be significantly inferior to the first one, indicating that Eq. (14) is violated.

A further important prediction of MCT is that the location of the minimum in the susceptibility for a given temperature is independent of the quantity. Comparing Figs. 11(b) and 11(c) we find this, within experimental error, to be the case for $\chi''_{s1}(k,\omega), k = 7$ and 13 for the A particles. However, if we compare $\omega_{\min}$ for χ''_{s1} and χ''_{s2} (see Figs. 11 and 21) we recognize that the two quantities differ by about a factor of 5. This is clearly larger than the numerical uncertainty for these values, indicating that the behavior of our system contradicts this prediction of MCT.

V. SUMMARY AND CONCLUSIONS

Before we present our conclusions of this work we offer a short summary of the main results.

By studying the van Hove self correlation function and the intermediate self scattering function we have found that our lattice-gas system, with hard-core interactions, exhibits very slow, temperature-dependent, nonexponential relaxation behavior at low temperatures. Note that the slowing down of the dynamics is observed for both kinds of particles, this despite the fact that at low temperatures about one-third of the A particles have a high mobility and relax therefore quickly. However, these fast particles should not influence significantly the relaxation behavior of the A particles for long times. Therefore it seems natural to investigate whether the predictions of MCT (or at least some of them) hold for both types of particles in our system. Although this theory was originally developed for simple liquids it was found experimentally that it also applies to much more complex systems, e.g., certain polymers (see, e.g., [15,23]). With this in mind the attempt to apply the theory to our system does not seem to be unreasonable.

An important step in testing the predictions of MCT is estimating the critical temperature T_c. We have tried to do this by investigating the following quantities: the diffusion constant D_B for the B particles, the relaxation times τ_A and τ_B for the intermediate scattering function F_{s1} for the A and B particles, respectively, the position $\omega_{\max}$ of the α peak in χ''_{s1} for A and B particles, the coefficient $\tilde{B}_{s1}$ of the von Schweidler law for A particles, the value of the susceptibility χ''_{s2} at $\omega_{\min}$ for the A particles, the energy per particle e_{tot}, and the value of the susceptibility χ''_{s1} at $\omega_{\max}$ for the A and B particles. Except for the last three quantities MCT predicts that all these quantities behave like a power law in the vicinity of T_c. In all cases we have found such a behavior, although in some cases the quality of the data is not good enough to exclude other fit functions. Thus having a theory in hand which predicts the analytical form of the fit function is of great value. Each fit gives T_c and a critical exponent γ, and in Table I we summarize our findings. From this table we estimate T_c to be 0.30 ± 0.03. The lowest temperature at which we think that we can do an equilibrium simulation for our system is 0.35. Thus using $T_c = 0.30$ the smallest $|\epsilon| = |T_c - T|/T_c$ is about 0.17. However, if we use the not unreasonable value of

TABLE I. Critical temperature and critical exponent for various quantities. The last column is the prediction of MCT for the critical exponent.

Quantity	T_c	Critical exponent	MCT
D_B	0.30	1.1	γ
τ_A	0.327	1.99	γ
τ_B	0.320	2.36	γ
$\omega_{\max A}$	0.25	1.0	γ
$\omega_{\max B}$	0.30 ± 0.02	1.7 ± 0.4	γ
$\tilde{B}_{s1}$	0.26	0.58	$\frac{1}{2} + \frac{b}{2a}$
$\chi''_{\min}$	0.26	0.63	0.5
$\chi''_{\max A}$	0.324	0.19	
$\chi''_{\max B}$	0.33 ± 0.02	0.24 ± 0.03	
e_{tot}	0.32	0.28	

$T_c = 0.32$ the smallest $|\epsilon|$ decreases to 0.09. Thus it does not seem unreasonable to assume that we are in the temperature regime where the asymptotic expressions of MCT for $|\epsilon| \to 0$ become valid. We found that the highest temperatures for which it was reasonable to do a power law fit are around 0.5–0.7 thus corresponding to an $|\epsilon|$ of order one. Although this value might seem too large to justify the application of asymptotic expressions, it is known from experiments that these formulas can be valid for such high values of $|\epsilon|$ (see, e.g., [15]).

Whereas T_c is determined quite well, this is not the case for the critical exponent γ. MCT predicts that the first five critical exponents in the table should all have the same value, but this is clearly not true. We have three values of about 2 and two which are close to 1. Whereas the former ones are comparable with values found in experiments [14–16] and computer simulations [24, 25], the latter ones are surprisingly small. However, these low values are not in contradiction with MCT since they are above the lower bound for γ of unity given by the theory.

The critical exponent for $\tilde{B}_{s1}$ is too small to be compatible with MCT, as the theory predicts it to be $\frac{1}{2} + \frac{b}{2a} > 1$. Also the critical exponent for $\chi''_{\min}$ shows a significant deviation from the MCT value of 0.5.

The last three entries in the table deal with quantities for which, to the best of our knowledge, MCT does not make any predictions. The critical exponents for these three entries are quite a bit smaller than the ones for the rest of the table. What is especially remarkable is the critical behavior of $\chi''_{\max}$. We are not aware of any place in the literature where experiments showing such a behavior have been reported.

In addition to the critical temperature and critical exponent, we have determined the von Schweidler exponent b for four quantities: χ''_{s1} for A and B particles, and χ''_{s2} for A (two kinds of fits) and B particles. The corresponding values are 0.50 ± 0.04, 0.73 ± 0.03 , 0.61, 0.99, and 0.55. Whereas a simple power law was employed to determine the first, second, and fifth of these exponents, the third and fourth were determined with the fitting function given in Eq. (26). The third value for the exponent was obtained by treating a and b as independent fit parameters and the fourth value by connecting a and b by the MCT relation in Eq. (6). The difference between the so obtained two values of b shows that the exact value of the exponent depends quite sensitively on the number of fit parameters used. Therefore our values reported for b might be subject to an appreciable systematic error. Thus it is difficult to decide if the above values for b are really compatible with the existence of a single value for b, but our results suggest that this is probably not the case. However, the fact that exponents b for χ''_{s1} for A and B particles are independent of temperature speaks in favor of MCT.

Our results for the Lamb-Mössbauer factor and the position of the minimum in the susceptibility give mixed results as tests for MCT. Although the k dependence of the nonergodicity parameter f_{s1} is in qualitative accordance with MCT, its temperature dependence is rather unusual. However, since our determination of f_{s1} is somewhat indirect and the predictions of MCT for this dependence are unclear to us, our findings are not necessarily in contradiction to the theory. More significant is the fact that the location $\omega_{\min}$ of the minimum in the susceptibility depends on the quantity under investigation, thus violating one of the predictions of MCT. In accordance with MCT Knaak found that $\omega_{\min}$ does not depend on the wave vector in the dynamic susceptibility of $Ca_{0.4}K_{0.6}(NO_3)_{1.4}$ [18]. The same result is found here as well, but we also find that $\omega_{\min}$ is not the same in χ''_{s1} and χ''_{s2}. Thus we think this to be a major contradiction with the theory.

The general version of MCT describes some situations in which some of the predictions stated in Sec. II no longer hold [9, 10]. These scenarios occur, for example, if the transition point is found to be in the vicinity of an end point of a transition line. As was shown by Götze and Haussmann, in the vicinity of such an end point the β-relaxation behavior becomes modified in that the power laws in t are replaced by logarithmic dependences [41]. Since we observe power-law behavior in the β-relaxation regime this kind of scenario can be ruled out. However, the same work also proposes another alternative for the transition: the line crossing scenario. The authors found that for such a scenario the β relaxation is still described by the two power laws, but for large, but not too large, times and for $\epsilon < 0$, $\Phi(t)$ behaves like $-|\epsilon| + \text{const} \times t^{-1/2}$, i.e., a power law plus a small *negative* constant. This is exactly the behavior we find for $F_{s1}(k,t)$, although in our case the exponent is -0.255. Thus, though we cannot be sure that our finding can be described by this second scenario proposed by Götze and Haussmann, it might very well be that a mechanism similar to the line crossing scenario is able to rationalize our results. A similar statement can be made about our findings on the critical behavior of the value of χ''_{s1} at $\omega_{\max}$. Flach, Götze, and Sjögren have proposed a scenario in which the amplitude of a peak in χ'' behaves critically [42]. However, this scenario would imply that there should be an additional peak at even lower frequencies and it is not clear whether this peak is not present or whether it is outside the frequency range accessible to our simulations.

Finally, it should be noted that there is another possible explanation of the discrepancies between our results and mode-coupling theory. As noted earlier, the predictions we have been testing are those of a theory that neglects the so-called phonon-assisted transport. Such transport is presumably possible in our model.

Before we end let us briefly examine the importance of the detailed dynamics of our model for the glasslike behavior observed and consider the likely effect of several modifications of the dynamics. To understand the importance of our dynamics, we must recognize that many of the attempted moves are rejected at very low temperatures. Since the collision part of the algorithm does not depend on temperature this means that between two successful moves the velocity of a particle will be randomized appreciably. Thus the dynamics at low temperatures will be similar to that of Metropolis Monte Carlo dynamics with single-particle moves. The same would be true if the branching ratio between the collision part and move part of the algorithm were to be increased. If, on the other

hand, this ratio were decreased the system would probably behave even more sluggishly than it does now since it will be harder for each particle to change its direction to move and will therefore be trapped more easily.

It is also interesting to compare our results to those obtained by Ajay and Palmer for their sliding block model [35]. They too find a relaxation behavior which for intermediate times behaves like a von Schweidler law. Their exponent is around 0.51, which is in agreement with a theoretical prediction by Brummelhuis and Hilhorst [43]. This is an additional indication that in lattice-gas models with hard-core interactions algebraic decays in the relaxation function can occur, thus giving further evidence for the broad applicability of MCT.

In summary, we have shown that, despite its simplicity, our hard-core lattice-gas model exhibits many of the dynamical phenomena observed in real glass formers. We have found that much of the behavior predicted by MCT is exhibited by the model, although many of the predictions seem to be only qualitatively correct (e.g., the existence of the von Schweidler law, the existence of various power laws, and the scaling behavior in the vicinity of the minimum of the susceptibility) rather than quantitatively correct (e.g., various critical exponents do not have the same value and the location of the minimum in the susceptibility is different for different susceptibility functions).

ACKNOWLEDGMENTS

We would like to thank S. J. Pitts for a careful reading of the manuscript and for many useful discussions. Part of this work was supported by the Swiss National Science Foundation, and by National Science Foundation Grant No. CHE89-18841. We made use of computer resources provided under NSF Grant No. CHE88-21737.

[1] K. Kawasaki, Phys. Rev. **150**, 291 (1966); Ann. Phys. (N.Y.) **61**, 1 (1970).

[2] W. Götze and M. Lücke, Phys. Rev. A **11**, 2173 (1975); J. Bosse, W. Götze, and M. Lücke, *ibid.* **17**, 434 (1978); **17**, 447 (1978); **18**, 1176 (1978).

[3] J. P. Boon and S. Yip, *Molecular Hydrodynamics* (McGraw-Hill, New York, 1980); J.-P. Hansen and I. R. McDonald, *Theory of Simple Liquids* (Academic, London, 1986).

[4] G. F. Mazenko, Phys. Rev. A **9**, 360 (1974); C. D. Boley, *ibid.* **11**, 328 (1975); G. F. Mazenko and S. Yip, in *Modern Theoretical Chemistry*, edited by B. J. Berne (Plenum, New York, 1977), p. 181; L. Sjögren, Phys. Rev. A **22**, 2866 (1980), and references therein.

[5] T. Geszti, J. Phys. C **16**, 5805 (1983); E. Leutheusser, Phys. Rev. A **29**, 2765 (1984); S. P. Das, G. F. Mazenko, S. Ramaswamy, and J. J. Toner, Phys. Rev. Lett. **54**, 118 (1985); T. R. Kirkpatrick, Phys. Rev. A **31**, 939 (1985).

[6] U. Bengtzelius, W. Götze, and A. Sjölander, J. Phys. C **17**, 5915 (1984).

[7] W. Götze, Z. Phys. B **60**, 195 (1985); L. Sjögren, Phys. Rev. A **33**, 1254 (1986); S. P. Das and G. F. Mazenko, *ibid.* **34**, 2265 (1986); W. Götze and L. Sjögren, J. Phys. C **20**, 879 (1987); K. H. Michel, Z. Phys. B **68**, 259 (1987); U. Krieger and J. Bosse, Phys. Rev. Lett. **59**, 1601 (1987); W. Götze and L. Sjögren, J. Phys.: Condens. Matter **1**, 4183 (1989); W. Götze and L. Sjögren, J. Phys.: Condens. Matter **1**, 4203 (1989); L. Sjögren, Z. Phys. B **79**, 5 (1990); S. P. Das, Phys. Rev. A **42**, 6116 (1990); J. S. Thakur and J. Bosse, *ibid.* **43**, 4388 (1991); M. Fuchs, W. Götze, I. Hofacker, and A. Latz, J. Phys.: Condens. Matter **3**, 5047 (1991); B. Kim and G. F. Mazenko, Phys. Rev. A **45**, 2393 (1992); J. Jackle and D. Sappelt, Physica A **192**, 691 (1993).

[8] W. Götze and L. Sjögren, J. Phys. C **21**, 3407 (1988).

[9] W. Götze, in *Liquids, Freezing and the Glass Transition*, edited by J. P. Hansen, D. Levesque, and J. Zinn-Justin, 1989 Les Houches Session LI (North-Holland, Amsterdam, 1991), p. 287.

[10] W. Götze and L. Sjögren, Rep. Prog. Phys. **55**, 241 (1992).

[11] *Dynamics of Disordered Materials*, edited by D. Richter, A. J. Dianoux, W. Petry, and J. Teixeira (Springer, Heidelberg, 1989).

[12] F. Mezei, W. Knaak, and B. Farago, Phys. Rev. Lett. **58**, 571 (1987); F. Fujara and W. Petry, Europhys. Lett. **4**, 921 (1987); P. N. Pusey and W. van Megen, Phys. Rev. Lett. **59**, 2083 (1987); B. Frick, D. Richter, W. Petry, and U. Buchenau, Z. Phys. B **70**, 73 (1988); F. Mezei, in *Dynamics of Disordered Materials* (Ref. [11]), p. 164; W. Doster, S. Cusack, and W. Petry, Phys. Rev. Lett. **90**, 1080 (1990); M. Elmroth, L. Börjesson, and L. M. Torell, *ibid.* **68**, 79 (1992).

[13] D. Richter, B. Frick, and B. Farago, Phys. Rev. Lett. **61**, 2465 (1988).

[14] E. Bartsch, M. Kiebel, F. Fujara, H. Sillescu, and W. Petry, in *Dynamics of Disordered Materials* (Ref. [11]), p. 135.

[15] B. Frick, B. Farago, and D. Richter, Phys. Rev. Lett. **64**, 2921 (1990).

[16] P. Taborek, R. N. Kleiman, and D. J. Bishop, Phys. Rev. B **34**, 1835 (1986); E. Bartsch, F. Fujara, M. Kiebel, H. Sillescu, and W. Petry, Ber. Bunsenges. Phys. Chem. **93**, 1252 (1989); J.-L. Barrat, W. Götze, and A. Latz, J. Phys.: Condens. Matter **1**, 7163 (1989); M. Fuchs, W. Götze, and A. Latz, Chem. Phys. **149**, 185 (1990); E. Rössler, Ber. Bunsenges. Phys. Chem. **94**, 392 (1990); L. Börjesson and W. S. Howells, J. Non-Cryst. Solids **131-133**, 53 (1991).

[17] W. Knaak, F. Mezei, and B. Farago, Europhys. Lett. **7**, 529 (1988).

[18] W. Knaak, in *Dynamics of Disordered Materials* (Ref. [11]), p. 64.

[19] W. van Megen, and P. N. Pusey, Phys. Rev. A **43**, 5429 (1991); W. van Megen, S. M. Underwood, and P. N. Pusey, Phys. Rev. Lett. **67**, 1586 (1991); W. Götze and L. Sjögren, Phys. Rev. A **43**, 5442 (1991); M. Kiebel, E. Bartsch, O. Debus, F. Fujara, W. Petry, and H. Sillescu, Phys. Rev. B **45**, 10301 (1992); D. L. Sidebottom, R. Bergman, L. Börjesson, and L. M. Torell, Phys. Rev. Lett. **68**, 3587 (1992).

[20] G. Li, W. M. Du, X. K. Chen, H. Z. Cummins, and N. J. Tao, Phys. Rev. A **45**, 3867 (1992).

[21] G. Li, W. M. Du, A Sakai, and H. Z. Cummins, Phys. Rev. A **46**, 3343 (1992).

[22] W. Petry, E. Bartsch, F. Fujara, M. Kiebel, H. Sillescu,

and B. Farago, Z. Phys. B **83**, 175 (1991).
[23] L. Sjögren, J. Phys.: Condens. Matter **3**, 5023 (1991).
[24] B. Bernu, J.-P. Hansen, Y. Hiwatari, and G. Pastore, Phys. Rev. A **36**, 4891 (1987); M. J. D. Brakkee and S. W. de Leeuw, J. Phys.: Condens. Matter **2**, 4991 (1990); H. Miyagawa and Y. Hiwatari, Phys. Rev. A **44**, 8278 (1991).
[25] J.-N. Roux, J.-L. Barrat, and J.-P. Hansen, J. Phys.: Condens. Matter **1**, 7171 (1989).
[26] G. F. Signorini, J.-L. Barrat, and M. L. Klein, J. Chem. Phys. **92**, 1294 (1989).
[27] G. H. Fredrickson and S. A. Brawer, J. Chem. Phys. **84**, 3351 (1986); W. Kob and R. Schilling, Phys. Rev. A **42**, 2191 (1990); S. Flach, J. Siewert, R. Siems, and J. Schreiber, J. Phys.: Condens. Matter **3**, 7061 (1991); J.-L. Barrat and M. L. Klein, Annu. Rev. Phys. Chem. **42**, 23 (1991); S. Flach and J. Siewert, J. Phys.: Condens. Matter **4**, L363 (1992); S. Flach and J. Siewert (unpublished).
[28] J.-L. Barrat, J.-N. Roux, and J.-P. Hansen, Chem. Phys. **149**, 197 (1990).
[29] H. Löwen, J.-P. Hansen, and J.-N. Roux, Phys. Rev. A **44**, 1169 (1991).
[30] W. Kob and R. Schilling, J. Phys.: Condens. Matter **3**, 9195 (1991); G. Wahnström, Phys. Rev. A **44**, 3752 (1991).
[31] U. Frisch, B. Hasslacher, and Y. Pomeau, Phys. Rev. Lett. **56**, 1505 (1986).
[32] *Lattice Gas Methods for PDE's*, Proceedings of the NATO Advanced Research Workshop held at the Center for Nonlinear Studies Los Alamos National Laboratory [Physica D **47**, Nos. 1 and 2 (1991)].
[33] S. J. Pitts and H. C. Andersen (unpublished).
[34] W. Ertel, K. Froböse, and J. Jäckle, J. Chem. Phys. **88**, 5027 (1988); J. Jäckle, in *Structure, Relaxation, and Physical Aging of Glassy Polymers*, edited by R. J. Roe and J. M. O'Reilly, MRS Symposia Proceedings No. 215 (Materials Research Society, Pittsburgh, 1991), p. 151.
[35] Ajay and R. G. Palmer, J. Phys. A **23**, 2139 (1990).
[36] G. Marsaglia and A. Zaman, Ann. Appl. Prob. **1**, 462 (1991).
[37] H. Bässler, Phys. Rev. Lett. **58**, 767 (1987).
[38] C. H. Reinsch, Num. Math. **10**, 177 (1967); C. H. Reinsch, *ibid.* **16**, 451 (1971).
[39] G. Buchalla, U. Dersch, W. Götze, and L. Sjögren, J. Phys. C **21**, 4239 (1988).
[40] S. Havriliak and S. Negami, J. Polymers Sci. Part C **14**, 99 (1966).
[41] W. Götze and R. Haussmann, Z. Phys. B **72**, 403 (1988).
[42] S. Flach, W Götze, and L. Sjögren, Z. Phys. B **87**, 29 (1992); S. Flach (private communication).
[43] M. J. A. M. Brummelhuis and H. J. Hilhorst, J. Stat. Phys. **53**, 249 (1988); Physica A **156**, 575 (1989).